Rita Pinto Marques
Bachelor in Micro and Nanotechnologies

FINE-HALE: mastering the physiochemical properties of Inhalation APIs

Dissertation submitted in partial fulfillment
of the requirements for the degree of
Master of Science in
Micro and Nanotechnologies Engineering

Adviser: Doctor Raquel Barros, Scientist, Hovione

Co-adviser: Doctor Elvira Fortunato, Full Professor, Faculdade de Ciências e Tecnologias, Universidade Nova de Lisboa

Examination Committee

Chairperson: Professor Doctor Rodrigo Ferrão de Paiva Martins
Raporteur: Doctor José António Ferreira Gamelas
Member: Doctor Ana Raquel Xarouco de Barros

FACULDADE DE CIÊNCIAS E TECNOLOGIA
UNIVERSIDADE NOVA DE LISBOA

September, 2019

FINE-HALE: mastering the physiochemical properties of inhalation APIs

“*You cannot teach a man anything;*
you can only help him to find it within himself.”

Galileo Galilei

Acknowledgements

Gostaria de começar por agradecer à Professora Dra. Elvira Fortunato e ao Professor Dr. Rodrigo Martins por terem criado este curso e por proporcionarem ótimas condições de trabalho e desenvolvimento.

Quero agradecer à Professora Dra. Elvira Fortunato pelas oportunidades que me proporcionou ao longo do curso e pela coorientação nesta tese de mestrado. Um enorme agradecimento à minha orientadora Dra. Raquel Barros pela forma como me recebeu na Hovione FarmaCiência SA, por tudo o que me ensinou e transmitiu, e pela forma como me orientou, que não só permitiu o meu desenvolvimento pessoal e intelectual como também garantiu que tivesse o acompanhamento necessário. Muito obrigada pela preocupação, pelas conversas e incentivo. Um agradecimento também ao Dr. Rafael Antunes, que em conjunto com a minha orientadora e coorientadora, me permitiu estagiar no grupo Research and Development Products da Hovione FarmaCiência SA.

À Sara Perico que foi a minha companheira de laboratório, e também de secretária. Com quem partilhei esta experiência e que me acompanhou nos meus dias de luta e nos meus dias de glória. Obrigada pela amizade Sara. Ao Joan, ao Bernardo, à Andreia e à Cíntia, obrigada pelos almoços e pelas gargalhadas.

À Sara Cardoso, pelo apoio incansável, por tudo o que me ensinou, pelo cuidado e disponibilidade constante. A tua ajuda foi imprescindível e valorizo-a muito. Obrigado também à Sara Sequeira pela simpatia e conselhos. À Luísa e ao Luís, à Cátia, à Susana, ao Sérgio e à Andreia. Ao João Caetano, ao João Alcântara e ao Filipe. Ao Salomão, ao Parreira e ao Pedro. Obrigada a todos os que constituem o grupo R&D e que de alguma forma contribuíram para o meu crescimento.

À equipa do CENIMAT, em especial à Sónia Pereira, Alexandra Gonçalves, Tomás Calmeiro, à Professora Daniela Gomes e à Professora Rita Branquinho.

À Maria, à Teresa e à Bárbara, pelo companheirismo, amizade e aventuras vividas ao longo do curso. Vocês marcaram este meu percurso. Obrigada ao Luís Pedreira, que não tem explicação científica. Obrigada ao Neto, o meu alentejano favorito. Obrigada ao João Vieira. Obrigado ao micro&nano 14/15.

À Mel, à Daniela, ao Rodrigo, ao João Miguel, ao António e ao Mourão por terem continuado a ser meus amigos ao longo destes 5 anos e por sempre me terem apoiado. Obrigada ainda ao Luís Oliveira, na qualidade de quase padrinho.

Ao Ricardo pela oportunidade que me deu e por acreditar em mim. Muito obrigada por tudo. Obrigada também ao resto da equipa, à minha Filipa, ao Zé, à Sóninha e à Rita.

À minha família que é tudo. Aos meus quatro avós. À minha mãe pelo carinho. Ao meu pai pela inspiração. À minha irmã por ser a minha melhor amiga.

Obrigada Duarte.

Obrigada a todos os que de alguma forma se cruzaram comigo neste percurso e contribuíram para a conquista desta etapa.

Resumo

A administração pulmonar de fármacos é uma das formas mais desejável de administração de fármacos para tratar doenças respiratórias e o sucesso dos inaladores de dose calibrada ou inaladores de pó seco, depende das propriedades da formulação. Estas propriedades estão relacionadas com as propriedades físico-químicas dos princípios ativos, que são influenciados pelo processo de micronização.

Esta tese teve como foco o melhoramento dos princípios ativos micronizados por uma técnica de moagem a húmido desenvolvida e patenteada pela Hovione FarmaCiência SA, (*Wet Polishing*), de forma a que estes tenham propriedades semelhantes às dos princípios ativos micronizados por moagem a seco, neste caso em específico, moagem por jato (*Jet Milling*). De modo a atingir esta finalidade, foi efetuada a seguinte caracterização: distribuição dos tamanhos de partículas por Sympatec; área específica de superfície através da técnica BET; densidade real por picnometria de hélio; cristalografia por difração de raio x em pó; análise térmica por calorimetria de varrimento diferencial; morfologia por microscopia de varrimento eletrónico; forças de adesão por microscopia de força atómica e energia de superfície por cromatografia gasosa inversa. Assim que as diferenças entre os dois tipos de materiais foram identificadas, foram aplicadas duas técnicas de modificação de superfície às partículas obtidas por WP: forno convencional e sistema de ultravioleta-ozono. As amostras modificadas foram também caracterizadas e por fim, o desempenho aerodinâmico foi investigado através de ensaios em FSIs.

Os resultados sugeriram que os tratamentos térmicos efetuados pelo forno convencional aumentam as irregularidades das superfícies das amostras, aproximaram as forças de adesão àquelas das partículas do grau M, não interferiram com a cristalinidade e comportamento térmico, e aumentaram a fluidez das formulações para inaladores de pó seco. Os resultados de BET foram considerados inconclusivos e o IGC não revelou diferenças nas componentes dispersivas da energia de superfície. Em suma, os resultados indicaram que o forno convencional é uma técnica promissora para a alteração das propriedades de superfície das partículas obtidas por WP, tornando-as mais semelhantes às partículas obtidas por JM.

Palavras-chave: Princípio ativo, moagem por jato, moagem a húmido, modificação de superfície, performance aerodinâmica.

Abstract

The pulmonary drug delivery is one of the most desirable ways of drug administration to treat respiratory diseases and the success of the MDIs or DPIs is dependent on the formulation properties. These properties are related with the physiochemical properties of APIs, which are influenced by the micronization process.

This thesis focused on the improvement of APIs micronized by wet milling, technique developed and patented by Hovione FarmaCiência SA., (Wet Polishing), in order to have similar properties to the APIs obtained from a conventional dry milling technique (Jet Milling). To achieve this, the following characterization was performed: PSD by Sympatec; surface area by BET; density by helium pycnometer; crystallography by XRPD; thermal analysis by DSC; morphology by SEM; adhesion forces by AFM and surface energy by IGC. Once the differences were identified between the two grades, two surface modification techniques were applied to the C grade particles: the conventional oven and UV-ozone irradiation. The modified samples were also characterized and afterwards, the aerodynamic performance tests were performed via FSIs.

The results suggested that the temperature treatment performed by conventional oven, increased the irregularities of the samples surfaces, approximated the adhesion forces to the ones of the Jet Milling particles, did not interfere with the crystallinity, thermal behavior and PSD, and enhanced the flowability of the formulations in DPIs. The BET results were considered inconclusive and IGC did not revealed significant differences in the dispersive component of surface energy. Summarizing, the results indicated that the conventional oven is a promising technique to change the surface properties of C grade particles, making them more similar to M grade particles.

Keywords: API, jet-milling, wet-polishing, surface modification, aerodynamic performance.

Contents

List of Figures

List of Tables

Acronyms

AFM	Atomic Force Microscopy
AIM	Abbreviated Impactor Measurement
API	Active Pharmaceutical Ingredient
APSD	Aerodynamic Particle Size Distribution
BET	Brunauer – Emmet – Teller
CAB	Cohesive – Adhesive Balance
CAPS	Capsules
DCM	Dichloromethane
DPI	Dry Powder Inhaler
DSC	Differential Scanning Calorimetry
ED	Emitted Dose
ETA	Ethyl Acetate
FPD	Fine Particle Dose
FPF	Fine Particle Fraction
FPP	Finished Pharmaceutical Product
FSI	Fast Screening Impactor
HPLC	High Performance Liquid Chromatography
HPMC	Hydroxypropyl Methylcellulose
IGC	Inverse Gas Chromatography
IP	Induction Port
JM	Jet Milling
MPA	Mouthpiece Adapter
NGI	Next Generation Impactor
OEB	Occupational Exposure Band
OEL	Occupational Exposure Limit
PDD	Pulmonary Drug Delivery
pMDI	pressurized Metered Dose Inhaler
PS	Pre-separator
PSD	Particle Size Distribution
SEM	Scanning Electron Microscopy
SSA	Specific Surface Area

TCM	Trichloromethane
THF	Tetrahydrofuran
UV	Ultraviolet
WHO	World Health Organization
WP	Wet Polishing
XRPD	X-Ray Powder Diffraction

Symbols

γ_1^d	Dispersive component of superficial tension of probe
γ_s^d	Dispersive component of surface energy
*AN**	Lewis acceptor number
DN	Lewis donor number of Gutmann
a	Molecular area of the probe
W_a^s	Specific component of work of adhesion

Prior Note

Throughout this document, due to confidentiality matters, the APIs in study will be mentioned by the code name instead of their actual composition and some of the bibliographic references will be omitted (every time it appears [see prior note]) when it is considered that presenting these references could lead to the identification of the APIs studied.

Motivation

The success of a formulation for inhalation (pMDI and DPI) is related with various parameters, such as physiochemical and interfacial properties of the active pharmaceutical ingredient (API): particle size, surface area, density, morphology, adhesive and cohesive properties, amorphous content and flow properties. These parameters are influenced by the micronization process and the ones used at Hovione FarmaCiência SA are jet milling (JM) and wet polishing (WP).

The WP technique is a patented technology by Hovione FarmaCiência SA and because it inputs less energy to break the particles it solves some problems that could occur with the JM process, such as the amorphization of the product and/or the conversion for a different crystalline form. It has also other advantages such as higher control of particle size reduction and its variability. However, it has been reported by clients, with focus on formulation for metered dose inhalers (MDI), that the particles obtained by WP process (with focus on API ST75C) presented a strong adhesion to the walls of the reactor or container which leads to a decrease in the formulation process yield, homogeneity and aerodynamic performance of the formulation.

Although the APIs addressed in this work have already been target of study, the knowledge acquired is mostly of its chemical properties and it is crucial to understand more about the physical properties. In order to make the WP the preferred size reduction method by the clients, there is the need to modify and improve the inhalation particles physiochemical and surface properties.

Objectives

The work developed in this thesis aims to achieve the improvement of the inhalation particles properties produced by WP, applying surface modification techniques that can be scaled up and used in batch production, by having similar properties to APIs micronized by JM. To understand which are the key properties that differentiate the API particles that were produced by JM (denominated M grades) and produced by WP (C grades) it is crucial to characterize the grades before and after the surface modification is performed. The characterization performed was the following: particle size distribution by Sympatec; surface area by BET; density by helium pycnometer; crystallography by XRPD; thermal analysis by DSC; morphology by SEM; adhesion forces by AFM and surface energy by IGC.

Once the differences were identified, two surface modification techniques were used: the conventional oven and UV-ozone irradiation. The modified APIs were then characterized with the previously used techniques to verify if the C grade modified samples presented similar properties to the M grade samples. Finally, to asses about the aerodynamic performance of the powders which showed their properties more similar to M grade and as proof of concept, FSIs assays were performed and API amount was quantified by HPLC.

Summarizing, the principal objectives of this program are:

- Develop a post-production treatment to particles that allow to obtain a better control of the desired particle properties;
- Contribute to the business strategy by acquiring knowledge on the manipulation of the properties of inhalation APIs and consequently present products with higher quality to company clients.

CHAPTER 1

Introduction

1.1 Pulmonary Drug Delivery

Nowadays, the pulmonary drug delivery (PDD) is one of the most common and desirable ways of drug administration to treat respiratory diseases (such as asthma, pneumonia and lung cancer) because the drug is deposited in the pulmonary region which has a large surface area, thin adsorption membrane and a good blood supply that allow a rapid systemic onset [1,2]. In Figure 1.1 is possible to observe the path of both carrier and drug in the respiratory system:

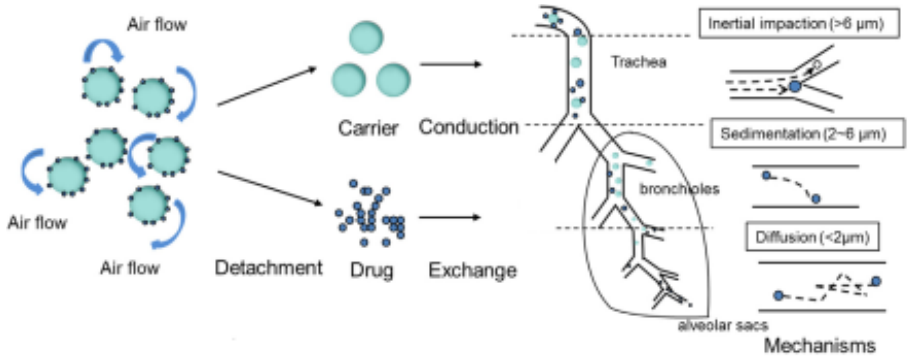

Figure 1.1: Deposition of an aerosol in the respiratory system for a dry powder inhaler. Adapted from [1].

The active pharmaceutical ingredients (APIs), according to the World Health Organization (WHO), can be defined as "any substance or combination of substances used in a finished pharmaceutical product (FPP), intended to furnish pharmacological activity or to otherwise have direct effect in the diagnosis, cure, mitigation, treatment or prevention of disease, or to have direct effect in restoring, correcting or modifying physiological functions in human beings." [3].

There are three main inhalation systems for the aerosolization of drugs: nebulizers, pressurized metered dose inhalers (pMDIs) and dry powder inhalers (DPIs). The nebulizers were the first inhalation systems developed where the drug is dissolved or suspended in a polar liquid, normally water and the liquid is atomized into small droplets [4–6]. As advantages, they do not use propellants and do not require special coordination between actuation and inhalation and due to this they are ideal for patients that have difficulties in using MDIs or DPIs. On the other hand, the compressors are heavy, noisy, require electricity or battery power, have limited portability, the administration can take from 5 to 30 minutes, is more expensive and need a more intense cleaning to prevent contamination [5–7]. In order to improve the quality of life of the patients, other devices have been developed which have higher efficiency, portability and shorter administration time [5].

An MDI consist on a drug formulation (drug substance dissolved or suspended in a propellant, mixture of propellants, or mixture of solvents, propellants, and/or other excipients) and a container closure system. The energy stored in a liquefied gas propellant under pressure generates aerosols for PDD [8]. In this type of devices it is crucial to coordinate the timing of the actuation and inhalation to achieve the proper therapeutic dose or otherwise some particles can be easily wasted because it is pressurized and emits the dose at high velocity [4,9,10].

DPI products are made of a drug formulation (contains the drug substance and excipients including a drug carrier, for example, lactose) and a container closure system [8]. This type of devices is activated by the patient's inspiratory airflow and for that reason they do not need the same coordination as for the MDI, but this can also be considered as a disadvantage because the deposition

efficiency is dependent on the patient's inspiratory airflow. However, because DPIs are made of dry powders and have a lower energy state, they have a reduced rate of chemical degradation, and they have more formulation stability [4].

1.2 Micronization

The API particles are conventionally manufactured to achieve a determined particle size, first by a crystallization process in which the API crystal are formed by adding an appropriate anti-solvent that will induce nucleation and the formation of the crystals, and then by a top-down size reduction technology to meet the product specifications [11,12].The size reduction process is crucial because the aerodynamic diameter for the delivery in airways is from 5 µm to 10 µm and in the deep lung it is from 1 µm to 5 µm. However, the size-reduction process can conduct to different physicochemical and interfacial properties of the APIs: particle size distribution (PSD), particle shape and rugosity, surface energy, cohesiveness, amorphous content and polymorphism. This parameters have influence on the formulation stability, interparticle interactions and on the aerodynamic performance of the drug product [11,13].

The milling or size reduction process is an operation where mechanical energy is applied to transform coarse particles into finer ones. There are various types of size reduction methods in the pharmaceutical manufacturing field such as: hammer mill, conical mill, ball mill, jet milling, wet polishing, amongst others [11, 14–16]. At Hovione FarmaCiência SA the main size reduction techniques used are jet milling (JM) and wet polishing (WP) which is a patent technology of the company. The decision about the method of milling the active pharmaceutical ingredients is based on the properties of the APIs and also on the client's requests.

1.2.1 Jet Milling

It is a very effective and standard technology for reducing particle size of API. In Figure 1.2 it is possible to observe a scheme of a spiral jet mill, like the one used in this work. There are two types of features that affect the grinding ratio: geometrical parameters like the diameter of the grinding chamber, shape, number and angle of grinding nozzles; operational parameters such as solid feed rate, grinding pressure, injector pressure and the input material [17].

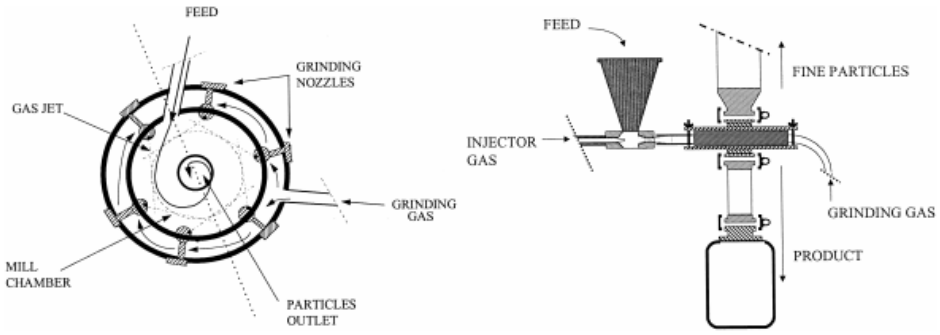

Figure 1.2: Scheme of a spiral jet mill [17].

In the milling chamber, the vortex motion of the particles and compressed air/nitrogen, promotes particle-to-particle collisions [18]. The breakage of particles occurs due to collisions between particles, and particles and walls, under the influence of opposing high velocity jets of compressed gas and the fine particles leave the system while the larger ones continue the comminution process [11,19].

Some of the principal strengths are the fact that it is a simple, cost effective and solvent free operation process; provides the appropriate particle size distribution for the inhalation formulations and can handle heat-sensitive materials. The drawbacks are the high input energy needed that can lead to amorphization, change in morphology and lead to chemical degradation; the resulting particles can be highly electrostatically charged and fractured crystals; the size, shape and morphology control is limited [18–20]. Consequence of the high energy input of the method, the surface of the crystal becomes damaged and local hot spots are generated. These sites can promote the formation of amorphous domains and a modification in the polymorphic form of the API. The micronization process also increases the particle surface energy and hence, leads to a higher cohesive behavior [11].

1.2.2 Wet Polishing

Wet polishing is a proprietary Hovione FarmaCiência SA technology and it was developed to solve some of the problems in JM, allowing the generation of a stable crystalline material which is dried by a spray drying process [21].

It consists in two combined technologies: one to achieve a small particle size and another to isolate the particles. In order to have a small particle size it can be used: a bottom-up technique (controlled crystallization or nanocrystallization) or a top down technique (high shear mixing or high-pressure homogenization). The isolation can be made in one step by spray drying or in two steps by filtration followed by a drying process. This way it is possible to meet specific drug delivery requirements [21]. Spray Drying (SD) is widely used in pharmaceutical industry and in Hovione FarmaCiência SA has been used to as a particle engineering technique mainly in the oral drugs field, but also for pulmonary particle engineering, to dry crystalline API and for encapsulation purposes [22,23]. SD consists in a feed (for example of a solution, emulsion or slurry) that is atomized into hot nitrogen conducting to evaporation of the liquid from the droplets and particle formation. These are separated in a cyclone or filter bag [22,24].

The main advantages of these two techniques combined are the optimal control over PSD, the narrow PSD spans, the particle customization (surface area and surface charge), can be scalable, the amorphization is reduced and the energy applied during the process is dispersed also to the liquid decreasing the stress in the particles. Nevertheless, it requires an appropriate anti-solvent, an isolation step and it can be challenging for thermally unstable compounds [11,21].

1.3 Formulation

1.3.1 DPI Formulation

The final drug product is a compromise between pharmaceutical, economic and engineering considerations. The formulation is one of the factors influencing the success of the product. A dry powder inhaler formulation consists in a blend of active pharmaceutical ingredients (APIs) and excipients. Most DPIs formulations are constituted by micronized APIs blended with large carrier particles because molecules with pharmacologic activity usually have poor physicochemical properties and this strategy allows an enhancement in flow, reduce aggregation and improve the dispersion [4].

The strategy addressed in this work is the carrier-based strategy, in which the micronized API is blended with an inert excipient, a coarse carrier, usually α-lactose monohydrate. In this approach, during the aerosolization, the API detaches from the carrier surface reaching the deep lung. The coarse particles are between 50 and 100 μm and lactose is the preferred carrier because it is compatible with the drug substance, have chemical and physical stability and is inexpensive. This

process is dependent on the cohesive – adhesive balance (CAB) between the drug particles and carriers [25–27]. It is important to achieve a balance between adhesive and cohesive forces in order to exist enough adhesion between drug and carrier to provide a stable formulation but not in excess to avoid a difficult separation during inhalation [26]. In order to optimize the drug delivery, a small amount of fine particle excipient denominated fines, normally lactose, can be aid to the formulation. This consists in a ternary formulation and it was the chosen strategy to produce the formulations investigated in this project. These lactose fines are in the range of 4 and 7 µm. The amount of fines in a formulation can vary between 1.5% and 10% and increases the FPD and FPF of the drug [28,29].

To produce a carrier-based DPI the API must be size reduced through a micronization technique (as it was discussed in section 1.2) and then blended with the excipients (Figure 1.3).

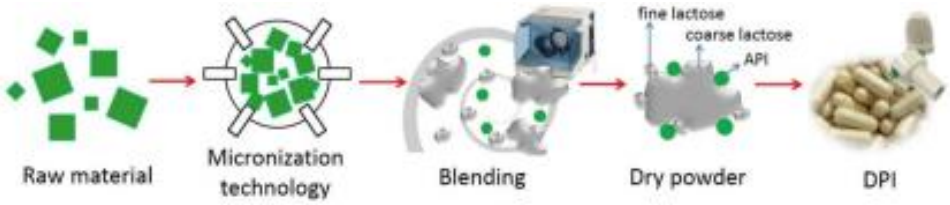

Figure 1.3: Schematic representation of the production of a carrier-based DPI [30].

1.3.2 Aerodynamic performance

It is very important to study the aerodynamic particle size distribution (APSD), i.e., where the particles in the cloud of an aerosol are deposited in the respiratory track, because it influences the therapeutic effect. For a faster and simpler screening of formulations usually is used in R&D the abbreviated impactor measurement (AIM) of the NGI preseparator, the Fast Screening Impactor, that separates the dose into coarse particle mass and fine particle mass. This was the chosen technique to simulate the track of DPIs formulations on our respiratory system. In Figure 1.4 is a schematic of the different components of an FSI, the mouthpiece adapter and the inhaler device. The induction port captures the non-inhalable particles as well the preseparator that has an insert that does a 5 µm cut-off diameter within a flow rate of 100 L/min [31].

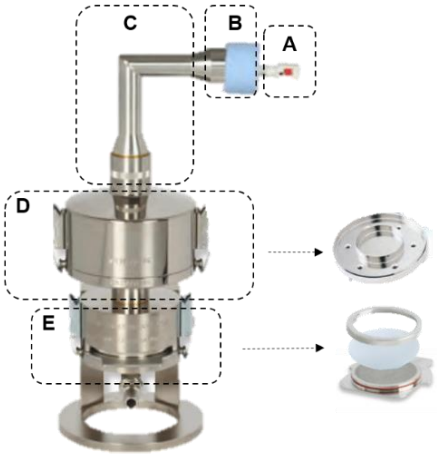

Figure 1.4: Fast Screening Impactor constituent: A – Inhaler device; B - Mouthpiece Adapter (MPA); C – Induction Port (IP); D – Preseparator (PS); E – Filter (Fil). Adapted from [32].

The particles larger than 5 µm are mostly impacted in the upper respiratory track; the particles in a range of 1 and 5 µm are deposited in the lower respiratory track (the bronchial tree and alveoli) and particles between 1 and 3 µm reach the alveolus tissue. The performance of the formulations can be assessed through impacting methods that simulate the track of the particles in the lungs, as referred previously, which allow the determination of the fine particle dose (FPD) that represents the amount of API that have an aerodynamic diameter below 5 µm, which are the particles that in theory can be deposited in the deep lung and have a therapeutic effect; the emitted dose (ED), i.e., the drug mass that exited the device and the capsules and that inform us about the ability of the powder to be fluidized by the device; and the fine particle fraction related with the emitted dose (FPF_{ED}) is the fraction between FPD and the ED [26]. The ED is influenced by the electrostatic deposition in the inhalers and mouthpieces, and differently charged particles could lead to particle agglomeration [33].

CHAPTER 2

Materials and Methods

This second chapter is divided in three parts. On the first part are presented the techniques that allowed the characterization of the original C and M grades of the two inhalation APIs in study and the modified ones; on the second part are presented the surface modification techniques applied to the C grade APIs, and lastly, on the third part are presented the assays that were done in order to conclude about the aerodynamic performance of the powders, both the original and the modified ones to ascertain if the properties changes conducted to an improvement of the formulation flowability properties.

For confidentiality matters the APIs in study will be mentioned by the code name instead of their actual composition. The input material consisted on two different APIs: ST75 and IH04. Both APIs were micronized by jet milling (M grade) and wet polishing (C grade). The identification of the products is made by internal codes: 05ST75M.HQ00298, 06ST75C.HQ00035, 05IH04M.HQ00004 and 05IH04C.HQ00003 (to simplify they will be mentioned throughout the document only by ST75/IH04 plus the C/M grade). The products were already micronized and so the size reduction process was not part of the techniques performed during the thesis. The micronization was made in Portugal by production or the research laboratories. These products are considered potents, i.e., have occupational exposure limits (OEL) bellow 10 µg/m^3 as an 8-hour time weighted average, and so they require special handling conditions. These APIs have a classification of occupational exposure band (OEB) of 3A (1 to 10 µg/m^3) [34].

2.1 Characterization of APIs

2.1.1 Scanning Electron Microscopy (SEM)

To assess about the particles shape and surface morphology was used the SEM-FIB – Zeiss Auriga CrossBeam Workstation with an accelerating voltage of 5 kV. All the samples were previously coated with iridium to achieve a 15 nm layer thickness. The characterization was made at CENIMAT|i3N FCT NOVA.

2.1.2 Particle Size Distribution (PSD)

The particle size distribution was evaluated by the laser particle size analyzer Sympatec HELOS/BR + RODOS/M + ASPIROS at Hovione FarmaCiência SA. This configuration is constituted by the modules presented in Figure A.1: HELOS/BR, the laser diffraction sensor that offers a size range of analysis from 0.1 µm to 8.750 µm (the size range is dependent on the lens that is being used, R1 to R5, and the choice of the lens is made based on a previously SEM analysis); the RODOS/M dry dispersion unit achieves an efficient and gentle dispersion of the samples through a compressed air injector that separates the particles; and ASPIROS, a micro dosing system where the sample vials are inserted. The system is closed avoiding contact between the samples and the surrounding environment. The measures are made for dry powder dispersions and this configuration allows a reliable examination even for agglomerative powders.

The powdery sample (a few to about 1 mg) must be in an appropriate vial and placed in the ASPIROS constituent. Then it is crucial that the dispersion conditions (pressure and velocity) and the lens chosen are the ones which will allow the better results. These parameters must be adjusted to the type of samples we want to study. The sample tube is opened in ASPIROS and the powder is aspirated into the RODOS injector in a free aerosol jet that is analyzed.

The PSD data (presented as Dv10, Dv50 and Dv90) of the input material is described in Table 2.1 and the PSD curves (volume-weighted distributions) are in Figure A.2 and Figure A.3. The M grade particles used have larger PSD than C grade.

The measurements were performed in triplicate. For IH04 (for both input and modified material) it was used the R1 lens, a pressure of 4 bar and a feed velocity of 50 mm/s and for ST75 (also for both input and modified material) it was used the R1 lens, a pressure of 5 bar and a feed velocity of 50 mm/s. The lens R1 was used because it has a range size of 0.18 µm - 35 µm.

Table 2.1: PSD data of IH04 and ST75 particles after the JM and WP process represented as the average of the measurements ± standard deviation (s.d.)

API	IH04M	IH04C	ST75M	ST75C
Dv10 (µm ± s.d.)	0.81 ± 0.02	0.60 ± 0.01	0.64 ± 0.01	0.57 ± 0.02
Dv50 (µm ± s.d.)	2.31 ± 0.05	1.54 ± 0.01	2.37 ± 0.06	2.00 ± 0.26
Dv90 (µm ± s.d.)	5.17± 0.09	3.15 ± 0.03	5.23 ± 0.07	5.09 ± 0.62

2.1.3 Specific surface area and true density

The specific surface area of the powders was obtained using a Micromeritics ASAP 2000 analyzer and the analysis gas was nitrogen. This technique determines the specific surface area of solids by gas adsorption using the Brunauer – Emmet – Teller (BET) theory. This analysis was made at Instituto Pedro Nunes.

To investigate the true density, it was used the Accupyc 1330 Pycnometer. It allows the determination of the occupied volume by an amount of material through the comparation between the variation of the helium at the chamber that contains the sample we want to analyze and the one of a calibrated volume chamber. This analysis was also made at Instituto Pedro Nunes. These results were only possible to obtain for the APIs IH04M, IH04C, ST75M and ST75C as shown in Table 2.2, due to the deadlines of the thesis. As it can be observed the product obtained from JM process is less dense than the one obtained from WP, for API IH04 but there are no significant differences for API ST75.

Table 2.2: True density and standard deviation of APIs IH04M, IH04C, ST75M and ST75C.

API	IH04M	IH04C	ST75M	ST75C
Density (g/cm^3 ± s.d.)	0.9363 ± 0.0267	1.2401 ± 0.0875	1.0089 ± 0.0506	1.0392 ± 0.0210

2.1.4 X-Ray Powder Diffraction (XRPD)

The X-ray diffractometer PANalytical's X'Pert PRO MRD provided information about the crystallographic structure of the APIs' powders. It was used the Bragg-Brentano geometry and the source of X-rays is Cu-Kα (λ=1.5406 Å). The generator voltage was 45 kV and the tube current 40 mA

The scan was made with a range of 2θ from 5° to 40° and a scan step size of 0.0167°. The characterization was made at CENIMAT|i3N FCT NOVA.

2.1.5 Differential Scanning Calorimetry (DSC)

Thermal analyzes were performed by DSC 250 Discovery from TA Instruments which had a refrigerated cooling system 40 (RSC40). The characterization was performed at Hovione FarmaCiência SA. The measurements were made from 0 °C to 350 °C with a ramping heat of 10°C/min. The samples were placed in an aluminum pinhole hermetic pan with weight between 3 and 6 mg and the equipment was calibrated previously with indium.

2.1.6 Atomic Force Microscopy (AFM)

Adhesion forces were measured by AFM Asylum MFP-3D Stand Alone (SA) in contact mode with an Olympus probe TR800PB long (K=0.16 N/m and F_0=22 kHz) which is made of silicon nitride and has a side gold coating. In order to immobilize the powder, the samples were prepared by embedding the powder on epoxy resin, and then the resin at the surface was polished so that the powder particles can be measured at the surface. This characterization was made at CENIMAT|i3N FCT NOVA.

2.1.7 Inverse Gas Chromatography (IGC)

The surface properties of the APIs were studied by inverse chromatography analysis using a DANI GC 1000 digital pressure control gas chromatograph at Universidade de Coimbra. The samples were packed on a stainless-steel column and analyzed at 52 °C. The substances injected were: methane, n-pentane, n-hexane, n-heptane, n-octane, cyclohexane, trichloromethane (TCM), dichloromethane (DCM), tetrahydrofuran (THF), ethyl ether, ethyl acetate (ETA) and acetone. Were made triplicate measurements.

2.2 Surface modification of APIs

The surface modification of APIs was performed by two techniques: the conventional oven by the J.P. Selecta, Vacuum drying oven Vaciotem-TV model (available in Hovione FarmaCiência SA) and UV - ozone irradiation by UV-ozone cleaner by Novascan PSD-UV (available in CENIMAT|i3N FCT NOVA). The vacuum oven presents a controllable temperature from 35 °C to 200 °C and they are calibrated to achieve a low variability and a high homogeneity.

The UV-ozone system has an UV light emitting grid (mercury vapor) that excites organic molecules producing a reactive ozone gas from the oxygen that is at the cleaning chamber. The wavelengths used are 185 nm and 254 nm. The conditions used are described in Table 2.3.

Table 2.3: Surface modification techniques and conditions used as post production treatment.

Conventional oven			UV ozone system	
Temperature (°C)	**Time point (h)**	**Relative humidity (%)**	**Time points (min)**	**Height of stage (cm)**
40	4, 8, 24	0	15	7.5
60			30	7.5
80			120	8.5

2.3 Aerodynamic performance

2.3.1 Formulation for DPIs

To evaluate about the aerodynamic performance of the APIs, lactose-based API formulations for dry powder inhalers (DPIs) were prepared with the following composition: 1% of API, 2.5% of fine lactose and 96.5% of coarse lactose. This part of the work was only done for the input APIs and for the APIs that were treated in the conventional oven for the 3 temperatures for 24 h (ST75C 40 °C, 60 °C and 80 °C during 24 h; IH04C 40 °C, 60 °C and 80 °C during 24 h), because these samples were the ones who presented a more highlighted change in its surface properties as it is shown in chapter 3. As fine lactose grade it was used the Lactohale 230 from DFE Pharma and as coarse lactose grade the Respitose SV003 also from DFE Pharma. The blends were done by the mixer Turbula T2F for 1 hour at 96 rpm (all the components were sieved through a 600 µm sieve) and each blend had 10 g. It was guaranteed a minimum of 24 hours of resting for all blends before HPMC capsules were filled manually with a weight of 30 mg. The aerodynamic performance evaluation was made on Hovione FarmaCiência SA.

2.3.2 Fast Screening Impactor (FSI)

It was used the FSI from Copley Scientific to assess the aerodynamic performance of the DPI formulations and to investigate the differences between the input APIs and the modified ones.

The filter used was an A/E glass fiber filter, 76 mm from Pall Corporation, and represents the lowest stages of the lungs, and hence the amount of API present in this stage determines the therapeutic effect of the drug. The device used was a Plastiape model RS01 and operated at 100 L/min at 4 kPa. The inhalation volume was of 4 L per actuation in all the assays because it is considered to be the normal forced inhalation capacity of an average sized male weighing about 70 kg [31]. In Figure A.4 is represented the flowmeter, flow controller and the vacuum pumps (all from Copley Scientific) that were used in the experiments. For each blend were carried out two replicates, and for each one it was actuated 4 capsules (for a period of 2.4 s each). The capsules were hand filled.

For each stage of the FSI equipment, the dissolution mixture is used to extract the powder. The amount of API deposited in each stage was quantified using high performance liquid chromatography. It was used the Waters Alliance e2695 HPLC System with Waters 2998 PDA detector (Figure A.5) and the software used to extract the results from chromatograms was Empower 3. It is a technique that allows the separation, identification and quantification of chemical substances in a mixture.

For all APIs it was used the same detection method:

- UV detector set for 240 nm;
- Retention time: ST75 – 9.024 min; IH04 – 3.012 min;
- Mobile phase: acetonitrile:methanol:ammonium acetate solution, pH=4, (35:35:30) by volume;
- Dissolution mixture: acetonitrile:water (50:50) + 0.05% phosphoric acid.

CHAPTER 3

Results and Discussion

Throughout this chapter it will be presented the experimental results and it is divided in two sections, the first one for the API ST75 and the second one for the API IH04. Each one of these parts is also divided in two other sub-sections: in the first it will be discussed the characterization of the original input material and also the modified one by different characterization techniques; in the second it will be presented the results that allow the assessment of the aerodynamic performance from the experiments obtained through the FSI.

Because some of the techniques can be very time consuming, not all the characterizations were performed for all the samples. Initially, SEM technique was used in order to investigate which were the most promising treatments in terms of surface modification. Afterwards, the samples chosen were characterized by the other techniques, with exception of the XRPD analysis that was made for all the samples.

3.1 Active Pharmaceutical Ingredient: ST75

The materials addressed in this section and their respective code name are in Table 3.1.

Table 3.1: Input and modified material referent to API ST75 and their code names.

Input material		
Micronization technique		**Sample code name**
Jet Milling		ST75M
Wet Polishing		ST75C
Modified material		
Treatment Conditions – Conventional Oven		**Sample code name**
Temperature: 40 °C / 60 °C / 80 °C	T. point: 4 h	ST75C 40 °C 4 h / ST75C 60 °C 4 h / ST75C 80 °C 4 h
	T. point: 8 h	ST75C 40 °C 8 h / ST75C 60 °C 8 h / ST75C 80 °C 8 h
	T. point: 24 h	ST75C 40 °C 24 h/ ST75C 60 °C 24 h/ST75C 80 °C 24 h
Treatment Conditions – UV ozone System		**Sample code name**
Height of stage: 7.5 cm	T. point: 15 min	ST75C 7.5 cm 15 min
Height of stage: 7.5 cm	T. point: 30 min	ST75C 7.5 cm 30 min
Height of stage: 8.5 cm	T. point: 120 min	ST75C 8.5 cm 120 min

3.1.1 Surface modification of API

Through the different characterization techniques performed for the ST75 and IH04 APIs, it was possible to identify which were the key properties that differentiated the M and C grade particles. Afterwards, using the surface modification techniques mentioned above one tried to approximate their characteristics.

Scanning Electron Microscopy (SEM)

The SEM images allowed to assess the shape of the particles and if the treatments were efficient on the change of the surface morphology. SEM is often used for qualitative analysis of the surface roughness [35]. In Figure B.1 at appendix B, it is possible to observe ST75 not micronized, i.e., the starting material before the micronization step. The particles shape varies but, in general, they all have sharp edges. It is important to compare the M and C grades in order to ascertain if the modified C grade samples are getting more similar to the M grade. In Figure 3.1 it can be observed that ST75M has a more wrinkled surface than ST75C, which has a more polished shape, with a smoother surface. It is known that the milling process can affect the particles surface properties [6]. Higher surface roughness means higher distance of separation between the drug particle and the carrier surface, or in this case, any relevant material surface (container, reactor, amongst others), which decreases the van der waals forces of attraction between them, adding more difficulty to the adhesion of APIs to these surfaces [35].

Taking this into account, the goal is to modify the C grade particles surface, so it become less smooth and have more asperities which decreases the contact area between surfaces. The SEM images of the APIs subjected to the conventional oven treatments at 40 °C, 60 °C and 80 °C (for 4 h, 8 h and 24 h), are shown in Figure B.2, Figure B.3 and Figure B.4, respectively. As the time of treatment increases, the roughness of the particles surfaces seems to increase too, with exception for the treatment at 80 °C, where the surface seems to be very similar for all the timepoints. This may be explained by the stabilization of the surface modification at higher temperature even if for a low duration treatment. For higher treatment temperatures, the particles surfaces showed an increase on their irregularities. This difference in morphology was more pronounced between the samples treated at 40 °C and the other two. The samples chosen as the most promising ones to continue the study and better understand how the surface properties change with temperature were the ones treated at 40 ºC, 60 ºC and 80 ºC during 24 h because a higher impact on the surface properties was observed (Figure 3.2).

The changes in the surface roughness of the particles subjected to the UV – ozone system are shown in Figure 3.3. The surface roughness increased with the decrease of the sample-source distance and with the increase of the exposure time (Figure 3.3a to Figure 3.3c). Despite this technique appears to effectively change the surface properties of APIs, the samples changed their color (normally white) to yellow. ST75 contain chromophore groups that absorb UV radiation and promotes chemical degradation and impurities growth. For this reason, no further characterizations were performed on these samples, except for XRPD.

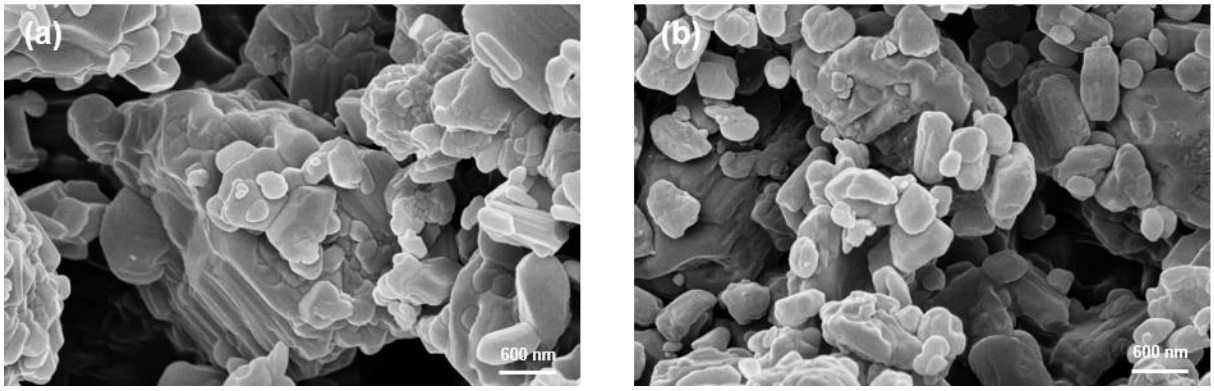

Figure 3.1: SEM images of input API (a) ST75M and (b) ST75C.

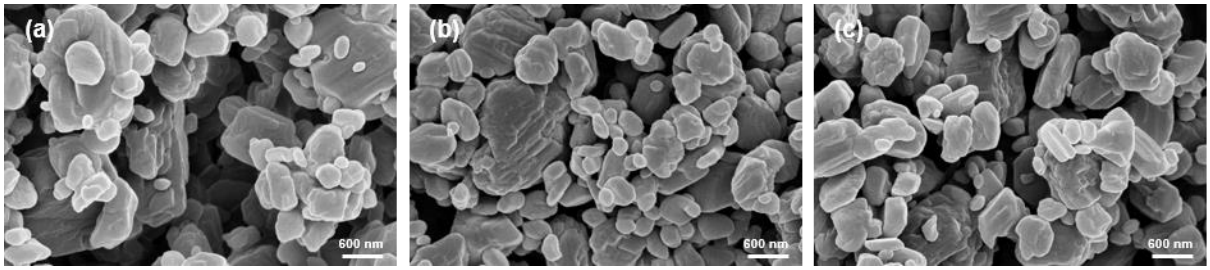

Figure 3.2: SEM images of the most promising modified samples by conventional oven: (a) ST75C 40 °C 24 h; (b) ST75C 60 °C 24 h; (c) ST75C 80 °C 24 h.

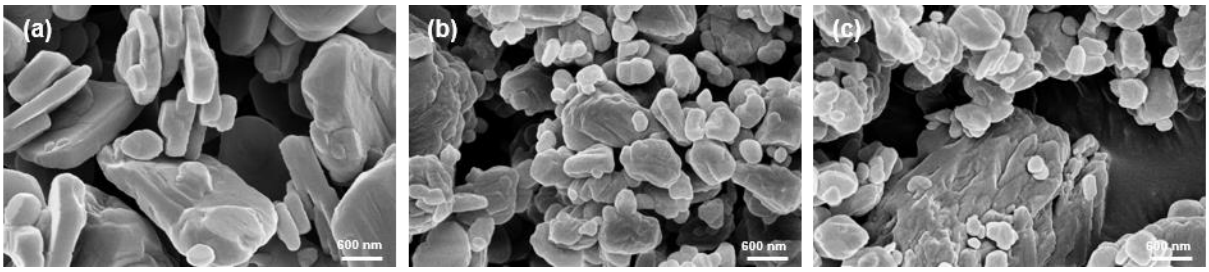

Figure 3.3: SEM images of samples treated in UV ozone system: (a) ST75C 7.5 cm 15 min; (b) ST75C 7.5 cm 30 min; (c) ST75C 8.5 cm 120 min.

Particle Size Distribution (PSD)

The particle size is an important parameter in the manufacturing process because it influences the flowability and delivery efficacy of the formulation [36]. In Figure B.5 are represented the PSD curves of ST75C and the 3 samples chosen previously to pursue the characterization study. They are considered normal distributions and don't exhibit the presence of different populations, that would result in an asymmetric curve. As it can be observed, on Figure 3.4, the PSD did not change with the treatment temperature. The fact the PSD of the modified samples remains the same as ST75C was a desired result.

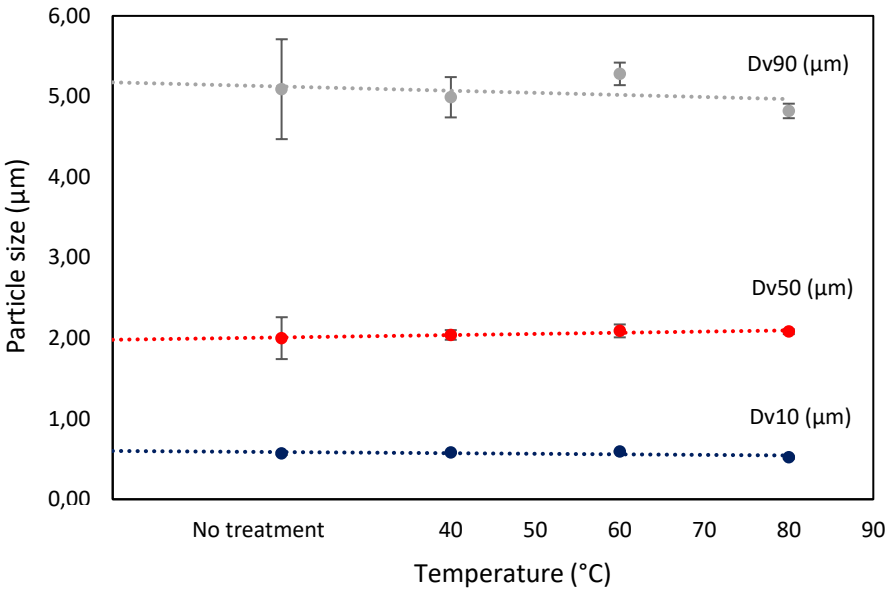

Figure 3.4: Dv10, Dv50 and Dv90, for ST75C with no treatment and with a treatment in conventional oven for 24 h at a temperature of 40 °C, 60 °C and 80 °C. The error bars represent the standard deviation based on n=3.

Specific surface area (SSA)

As an indirect measure of surface roughness, the specific surface area by nitrogen adsorption using the BET method was evaluated. This method was chosen over the AFM surface topography due to the features of the particles in study, that are rough and difficult the measurements in AFM that are considered ideal to smoother particles [35].

ST75C presented a higher specific surface area (SSA) than ST75M (Figure 3.5). It was expected that ST75C would have a lower SSA due to its smoother surface according to the SEM images [see prior note]. However, specific surface area results for other batches of ST75M revealed higher values of SSA (~10 m^2/g), suggesting this is an atypical batch, or it could be related with experimental errors. This method has an equipment error of ± 1 m^2/g and since the values of SSA obtained were very low the analysis was inconclusive. In order to overcome the challenges resulting from this method, other techniques could have been used to determine the surface rugosity such as laser profilometry [37].

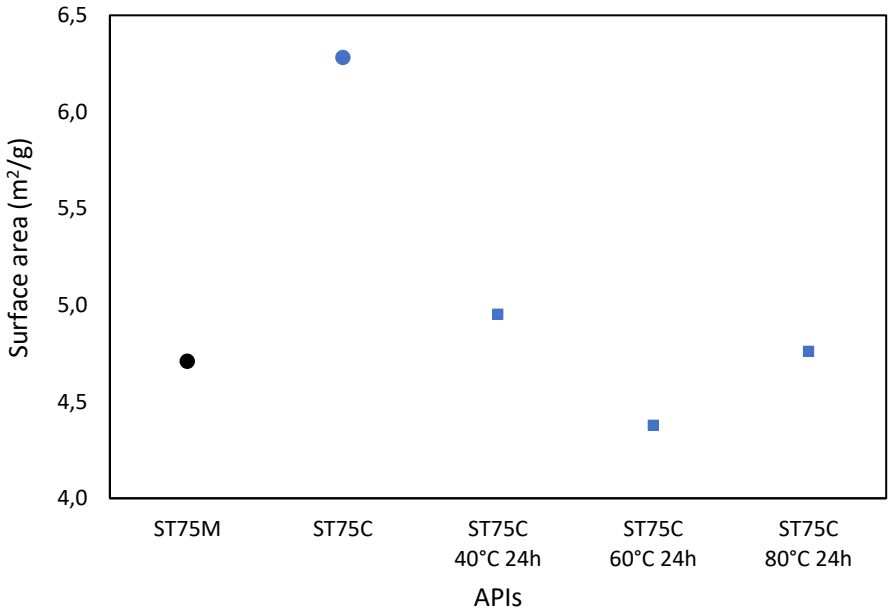

Figure 3.5: Specific surface area obtained by BET for ST75M, ST75C and ST75C 40 °C 24 h, ST75C 60 °C 24 h and ST75C 80 °C 24 h.

X-ray Powder Diffraction (XRPD)

The XRPD analysis was done in order to investigate the influence of the temperature treatment on the crystallinity of the materials produced. It is of great importance the evaluation of crystal polymorphs and crystallinity because they have influence on the stability of the formulation and on the therapeutic effect [38].

From the diffractograms presented on Figure 3.6, and in Figure B.6, Figure B.7, Figure B.8, Figure B.9 it was possible to state that ST75M, ST75C and all the samples treated with the conventional oven at different temperatures and time points, and also the UV-ozone system samples, do not show significant differences in terms of crystallinity and polymorphic form. The samples presented similar sharp diffraction peaks at the same 2θ angles, meaning that the APIs are crystalline and have the same polymorphism. These XRPD diffractograms are similar to those found in literature [see prior note].

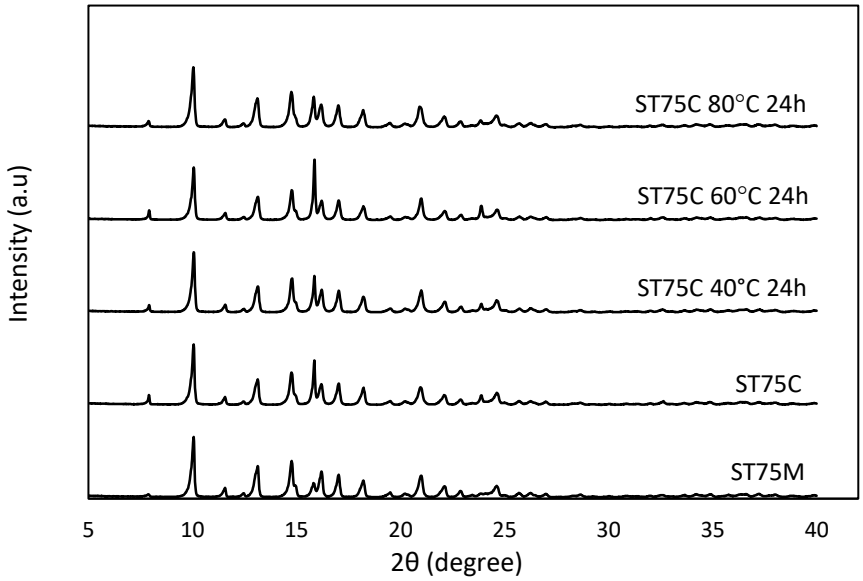

Figure 3.6: X-Ray diffractograms of ST75M, ST75C, ST75C 40 °C 24 h, ST75C 60 °C 24 h and ST75C 80 °C 24 h.

Differential Scanning Calorimetry (DSC)

Since the temperature used during the treatment could affect the polymorphism and crystallinity it was considered important to study the thermal behaviour [38]. In order to evaluate the thermophysical properties of the APIs, it was used the DSC technique.

The thermograms displayed in Figure 3.7 presented an endothermic peak at ~287 ºC, that corresponds to the melting point, and an exothermic peak at ~300 ºC indicating degradation of the product. This indicates that ST75M and ST75C only degrade above that temperature. All the treated samples (Figure 3.7c, d and e) presented thermograms similar to the one of ST75C meaning that the polymorphism and crystallinity were not affected with the temperature of the treatment. These results are in accordance with literature [see prior note].

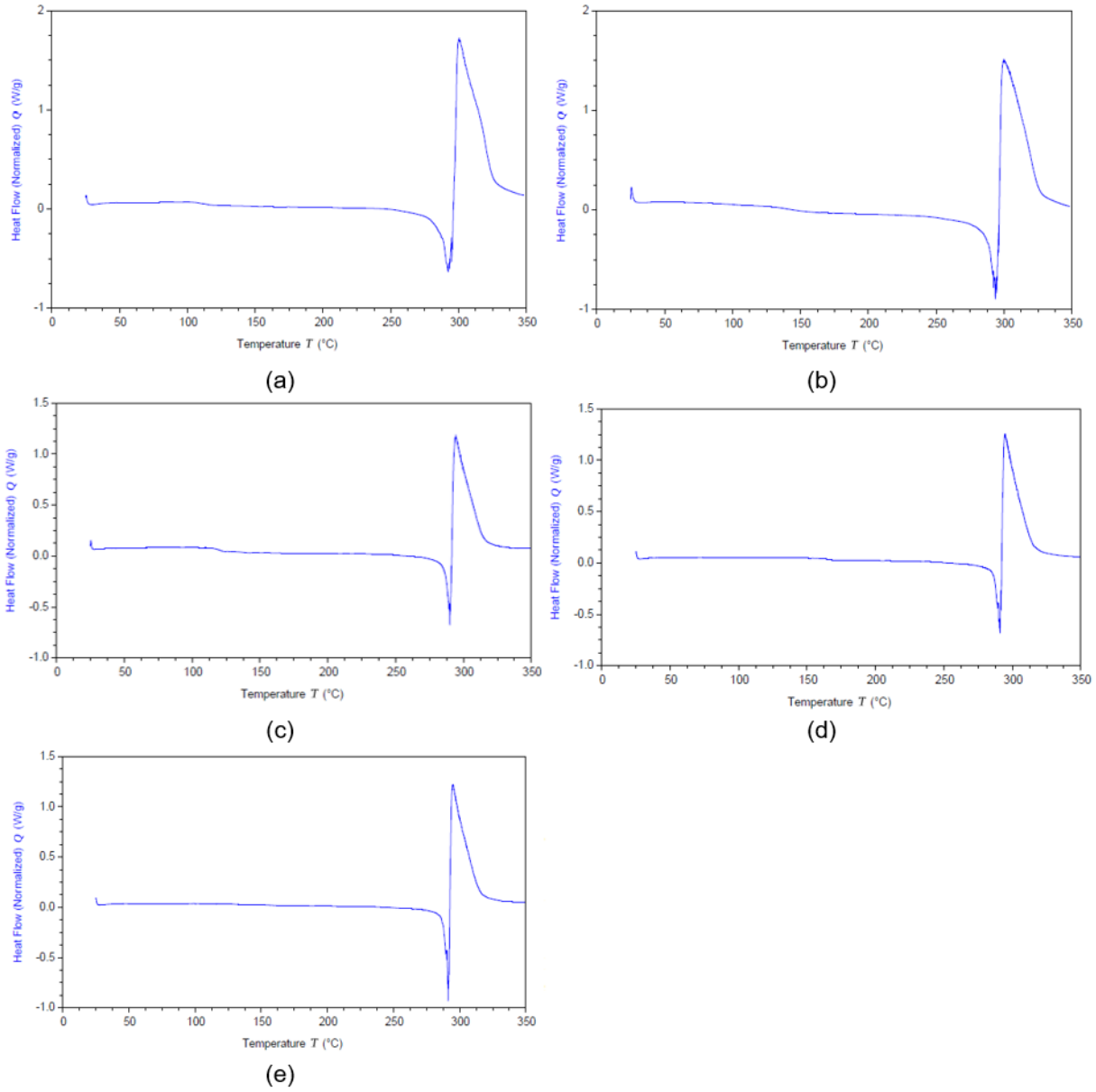

Figure 3.7: Differential scanning calorimetry thermograms of (a) ST75M; (b) ST75C; (c) ST75C 40 °C 24 h; (d) ST75C 60 °C 24 h; (e) ST75C 80 °C 24 h.

Atomic Force Microscopy (AFM)

The adhesion forces (pull-off) were obtained by the force *vs* distance curves from AFM. Figure 3.8 indicates that ST75C has higher adhesion force than ST75M which is accordant with the SEM images and literature: a rougher surface has less adhesion force since the surface roughness decreases the contact area between solid bodies since only the surface asperities come into contact and consequently the adhesion decreases [40]. The modified samples presented a decrease in the adhesion forces when compared to ST75C, getting more similar to ST75M, as desired. The fact that the standard deviation was large did not allow to identify which sample approximated more to the ST75M results. The AFM technique presented a large deviation between measurements and suggested a low reproducibility. In order to ascertain if AFM is a reliable technique to study these powders, more measurements should be performed.

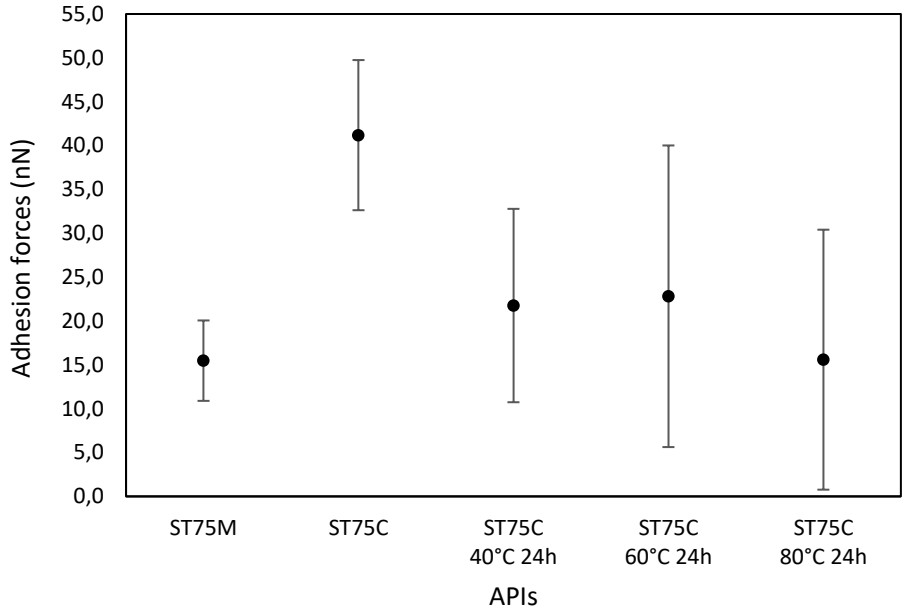

Figure 3.8: Average adhesion forces measured by AFM for API ST75M, ST75C, ST75C 40 °C 24 h, ST75C 60 °C 24 h and ST75C 80 °C 24 h. The error bars represent the standard deviation of all the measurements made on 3 different spots of the sample.

Inverse Gas Chromatography (IGC)

Inverse gas chromatography is one of the preferable techniques to investigate the surface energy of powders, over other techniques such as contact angle measurements that have problems related to the roughness and porosity of the samples [41]. IGC allows to acquire knowledge about the dispersive component of the surface energy (γ_s^d), related with long range forces such as van der Waals, through the measurements with alkanes, and the Lewis acid-base properties based on calculation of specific component of work of adhesion (W_a^s) [41].

The properties of the probes used for calculating the IGC parameters are presented in Table 3.2. The IGC results of dispersive component of surface energy (γ_s^d) and specific component of work of adhesion (W_a^s) are in Table 3.3. The specific component of work of adhesion for the ETA probe was not possible to measure due to its strong interaction with the samples, and consequently its high retention time. It is possible to conclude that are no significant differences between dispersive components of surface energy for the 5 samples, once the error associated to the measurements is 2 mJ m^{-2} and the values are all close to each other, not pointing to any tendency. All powders showed a stronger interaction with the amphoteric probe (acetone), suggesting they have a amphoteric behavior, i.e., they can interact as acid or base [42]. This confirm the strong interaction between the samples and the ETA probe which also has an amphoteric character. After the acetone probe, the samples showed higher affinity to basic probes (THF and ethyl ether), revealing their acid character. This is confirmed by the ratio between W_a^s (THF) and W_a^s (TCM), shown in Table 3.3, that presented high values. It was not possible to sustain that the modified powder became more similar to M grade based on the results obtained with IGC technique.

Table 3.2: Properties of the probes used for calculating the IGC parameters. *a* corresponds to molecular area of the probe; γ^d its the dispersive component of surface tension of probe; *DN* its Lewis donor number of Gutmann and *AN** it's the acceptor number of Lewis.

Probe	Type	*a* ($Å^2$)	γ^d (mJm^{-2})	*DN* (KJ mol^{-1})	*AN** (KJ mol^{-1})
n-pentane	apolar	46.1	16.0		
n-hexane	apolar	51.5	18.4		
n-heptane	apolar	57.0	20.3		
n-octane	apolar	63.0	21.3		
TCM	acidic	44.0	25.0	0	22.7
DCM	acidic	40.0	27.6	0	16.4
THF	basic	45.0	22.5	84.4	2.1
Ethyl ether	basic	47.0	15.0	80.6	5.9
ETA	amphoteric	48.0	19.6	71.8	6.3
Acetone	amphoteric	42.5	16.5	71.4	10.5

Table 3.3: Dispersive component of surface energy (γ_s^d, mJ m^{-2}) and specific component of work of adhesion (W_a^s, mJ m^{-2}) of polar probes (Lewis acid-base).

API	γ_s^d	W_a^s (TCM)	W_a^s (DCM)	W_a^s (THF)	W_a^s (Ethyl ether)	W_a^s (Acetone)	THF/ TCM
ST75M	53.0±2	1.4±0.7	9.3±0.6	23.1±0.4	21.3±0.2	40.6±0.6	16.5
ST75C	52.5±2	3.0±0.7	6.5±1.0	21.7±1.0	19.4±0.3	36.7±0.5	7.2
ST75C 40 °C 24 h	54.6±2	3.0±0.3	5.1±0.4	22.2±0.1	18.9±0.1	36.8±0.3	7.4
ST75C 60 °C 24 h	52.1±2	1.0±0.1	4.9±0.9	20.2±0.2	18.4±0.1	35.0±0.9	20.2
ST75C 80 °C 24 h	53.8±2	3.5±0.3	6.0±0.4	21.2±0.6	19.9±0.1	35.3±0.4	6.1

3.1.2 Aerodynamic performance

After the surface modification step and after performing the characterization of the materials obtained, it was important to confirm if these changes on the surface properties that approximated the properties of grade C to grade M (conclusion suggested by SEM and AFM), were also reflected on the aerodynamic performance. The in vitro aerodynamic performance was assessed by a Fast Screening Impactor, measuring the fine particle dose (FPD), i.e., the mass deposited in the filter; the content in each stage; the emitted dose (ED) which corresponds to the sum of the content deposited in all stages except for the device and capsules; and the fine particle fraction over the emitted dose (FPF(ED)) that is the fraction between FPD and ED [26].

Figure 3.9 and Figure 3.10 provide information regarding the FPF and FPD results. ST75M presents a higher FPF and FPD than ST75C, meaning that it was easier for API ST75M to detach from the carrier and achieve the filter of the FSI, having better flowability. The FPF of the modified samples increased when comparing with ST75C non modified, becoming more similar to the one obtained with the grade M. This indicates that the temperature treatment was successful in improving the aerodynamic performance of the powders. The FPD of the modified samples is similar to the one of ST75C, except for ST75C 60 °C 24h. Sample ST75C 60 °C 24h has the lower FPD and FPF but has also a big standard deviation. The large standard deviations of the FSIs measurements can be related to the small number of replicates (only 2) due to the amount of time required to each measurement.

The emitted dose of ST75M is slightly lower than the one of ST75C (Figure 3.11) and decreased a lot for the modified samples. It was expected that the emitted dose of the samples which showed a higher FPD and so a better flowability, would have detached more easily from the capsules. However, because the capsules were hand filled and due to the lack of experience in this process, could have been introduced error and this could have influenced the detachment of the powder from the capsule, affecting the ED.

In Figure 3.12 is possible to ascertain in which stages the API was deposited and observe the content deposited at the filter, which represents the lowest stages of the lungs and also mentioned as FPD.

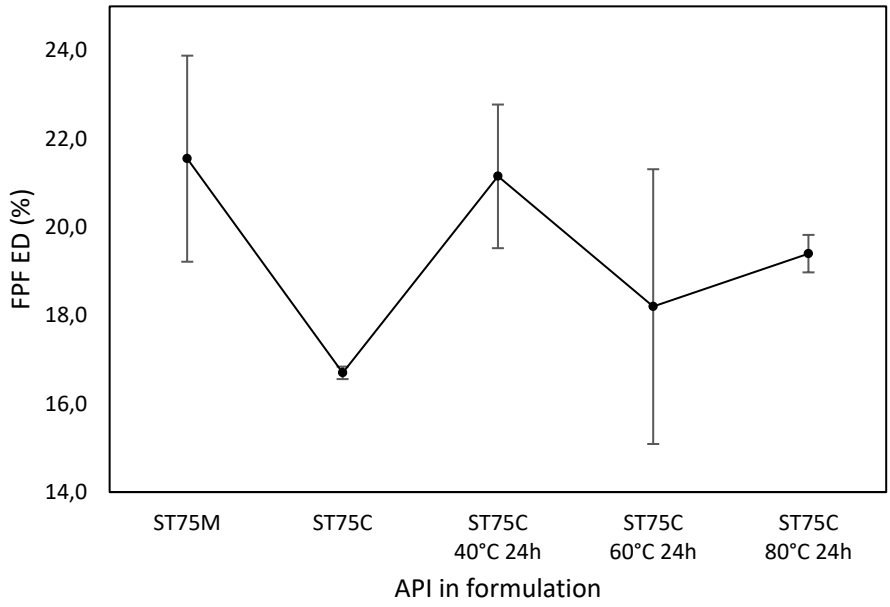

Figure 3.9:Aerodynamic performance evaluation through the FPF (ED) for the blends with the API ST75M, ST75C, ST75C 40 °C 24 h, ST75C 60 °C 24 h and ST75C 80 °C 24 h. The error bars represent the standard deviation based on n=2.

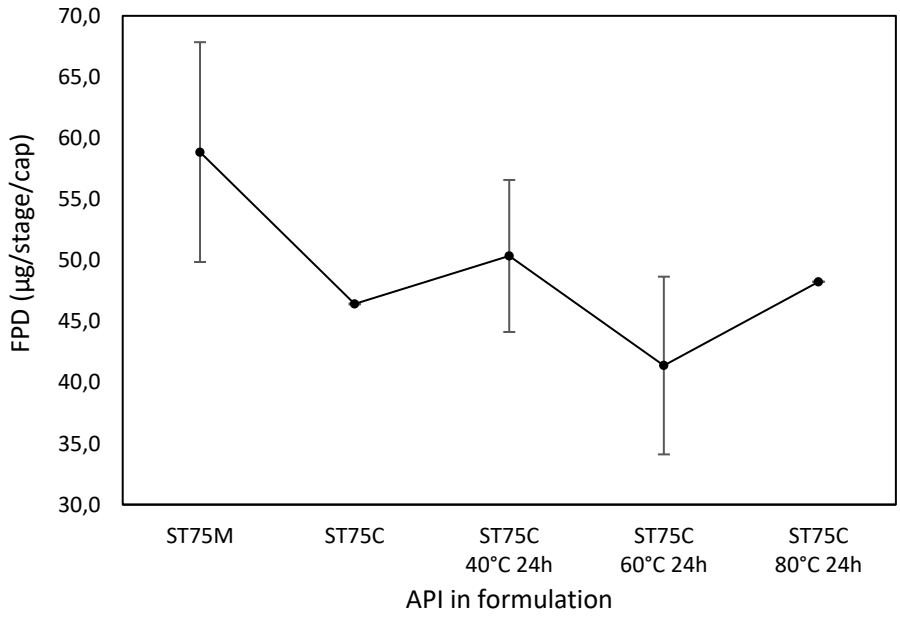

Figure 3.10: Aerodynamic performance evaluation through FPD for the blends with the API ST75M, ST75C, ST75C 40 °C 24 h, ST75C 60 °C 24 h and ST75C 80 °C 24 h. The error bars represent the standard deviation based on n=2.

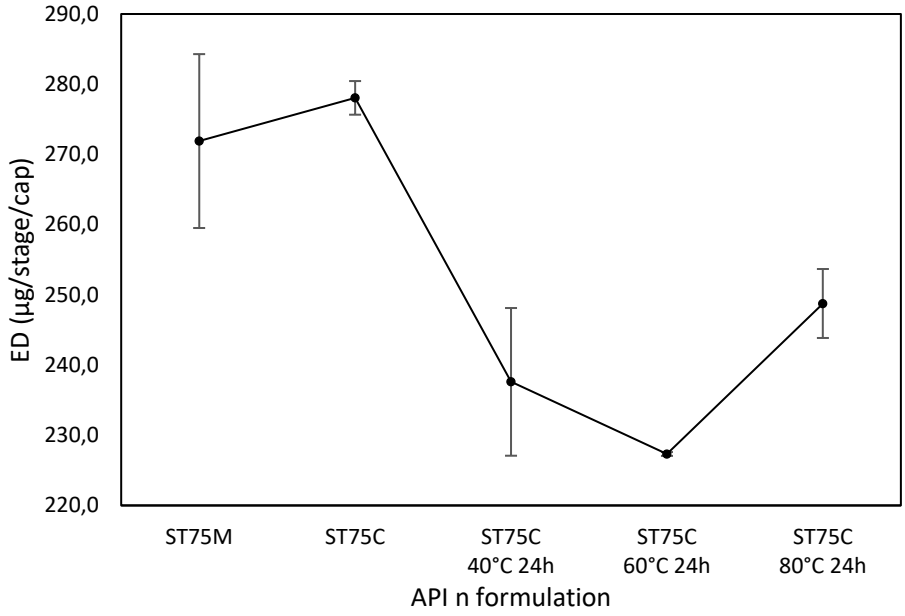

Figure 3.11: Aerodynamic performance evaluation through the ED for the blends with the API ST75M, ST75C, ST75C 40 °C 24 h, ST75C 60 °C 24 h and ST75C 80 °C 24 h. The error bars represent the standard deviation based on n=2.

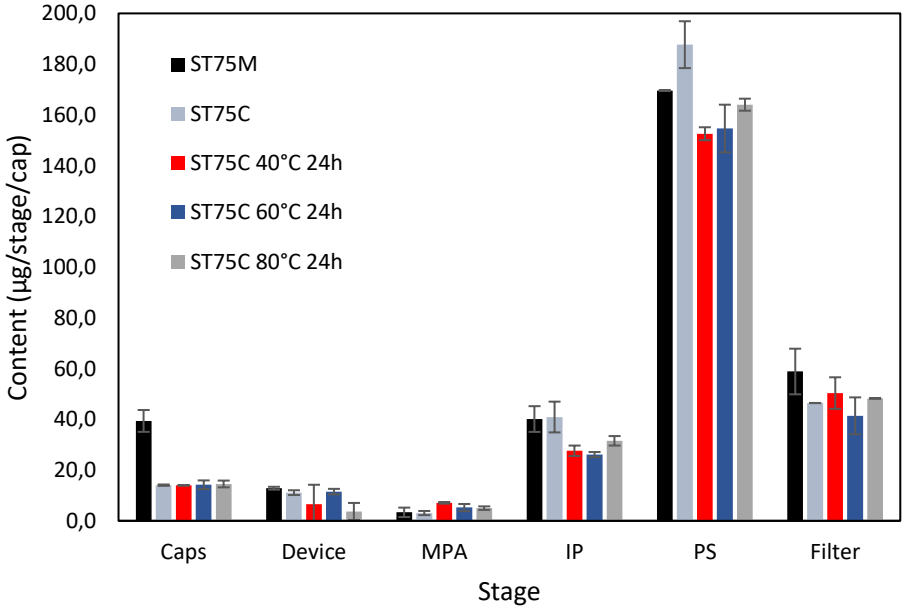

Figure 3.12: Aerodynamic performance evaluation through the content in each stage of the FSI for the blends with the API ST75M, ST75C, ST75C 40 °C 24h, ST75C 60 °C 24h and ST75C 80 °C 24h. The error bars represent the standard deviation based on n=2.

3.2 Active Pharmaceutical Ingredient: IH04

The materials used in this section and their code names are presented on Table 3.4. The surface treatments performed were similar to those used for ST75.

Table 3.4: Input and modified material referent to API IH04 and their code names.

Input material		
Micronization technique		**Sample code name**
Jet Milling		IH04M
Wet Polishing		IH04C
Modified material		
Treatment Conditions – Conventional Oven		**Sample code name**
Temperature: 40 °C / 60 °C / 80 °C	T. point: 4 h	IH04C 40 °C 4h / IH04C 60 °C 4 h / IH04C 80 °C 4 h
	T. point: 8 h	IH04C 40 °C 8h / IH04C 60 °C 8 h / IH04C 80 °C 8 h
	T. point: 24 h	IH04C 40 °C 24h/ IH04C 60 °C 24 h/ IH04C 80 °C 24 h
Treatment Conditions – UV Ozone System		**Sample code name**
Height of stage: 7.5 cm	T. point: 15 min	IH04C 7.5 cm 15 min
Height of stage: 7.5 cm	T. point: 30 min	IH04C 7.5 cm 30 min
Height of stage: 8.5 cm	T. point: 120 min	IH04C 8.5 cm 120 min

3.2.1 Surface modification of API

Scanning Electronic Microscopy (SEM)

In Figure B.10 it is possible to observe IH04 non micronized, i.e., the starting material before the micronization step. It presented a plated and chipped shape. When comparing the micronized samples, it can be observed that IH04M has more irregularities in its surface and has shaper edges than IH04C which has more spherical particles with a smoother surface (Figure 3.13), although the differences in rugosity are not as evident as in ST75. The statements done about the roughness for ST75 in Surface modification of API, applies to IH04 too: an higher surface roughness means higher distance of separation between the drug particle and the carrier surface, or any relevant material surface which decreases the van der waals forces of attraction between them, adding more difficulty to the adhesion of APIs to these surfaces [35].

Similarly to ST75, the SEM images of the APIs subjected to the conventional oven treatments at 40 °C, 60 °C and 80 °C (for 4 h, 8 h and 24 h) in Figure B.11, Figure B.12 and Figure B.13 suggested that the irregularities in particles surfaces increases with the time of treatment, except for IH04C 40 °C 4 h that appears to have a more shriveled surface than the others time points for 40 °C. This could be related with some event at the time of this treatment. For higher treatment temperatures, the particles

surfaces showed a slightly increase on their irregularities. To proceed with the surface characterization, it were chosen the samples with higher time point for all the temperature treatments, since it was observed a higher impact on the surface properties (Figure 3.14).

Although the changes in the surface roughness of the particles subjected to the UV – ozone system were not as pronounced as for ST75 one can still observe its impact as shown on Figure 3.15. Because the samples displayed a change in their color (from white to yellow) and contain chromophore groups that absorb UV radiation and promotes chemical degradation and impurities growth, no more characterizations were performed on these samples, except for XRPD.

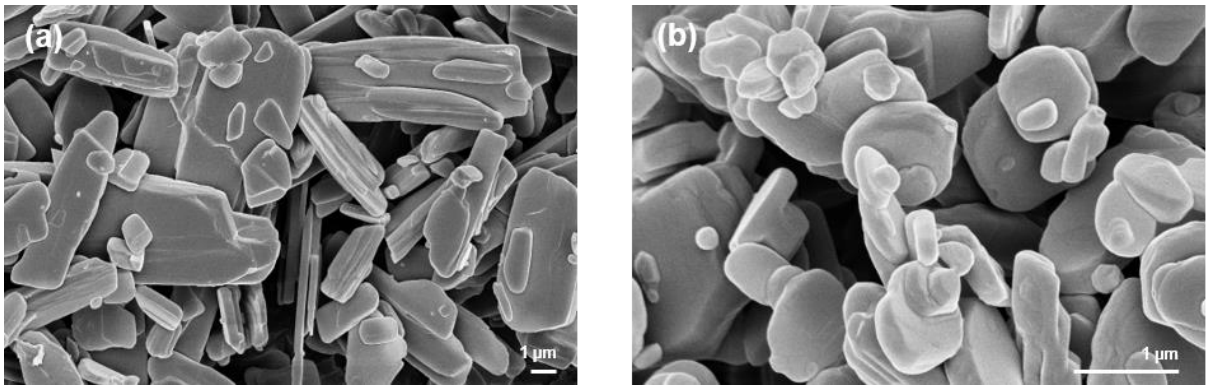

Figure 3.13: SEM images of input API (a) IH04M and (b) IH04C.

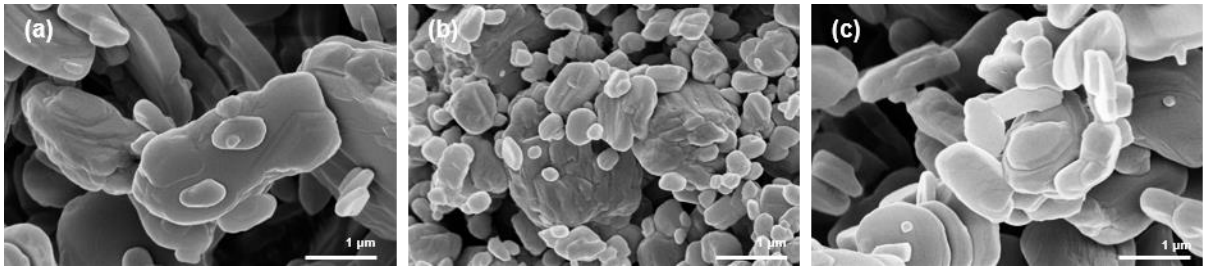

Figure 3.14: SEM images of the most promising modified samples by conventional oven: (a) IH04C 40 °C 24 h; (b) IH04C 60 °C 24 h; (c) IH04C 80 °C 24 h.

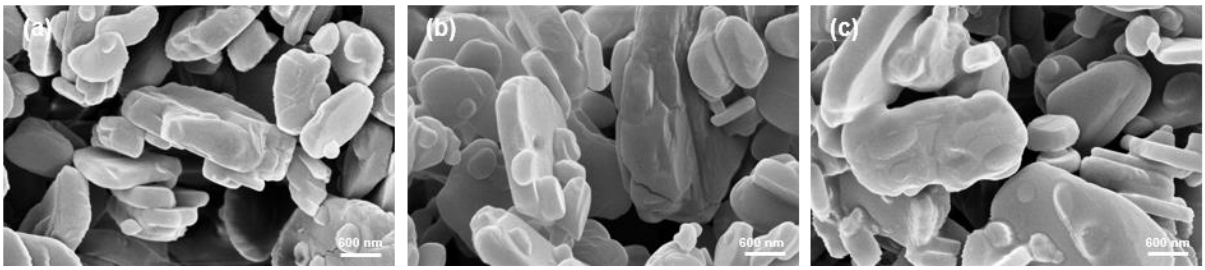

Figure 3.15: SEM images of samples treated in UV Ozone system: (a) IH04C 7.5 cm 15 min; (b) IH04C 7.5 cm 30 min; (c) IH04C 8.5 cm 120 min.

Particle Size Distribution (PSD)

Similarly to ST75, it can be observed that the PSD remained constant independently of the treatment temperature. This was a great result since the finality was only to change the surface properties of the APIs.

In Figure 3.16 Dv90 trend line exhibit a small decrease with treatment temperature but it was not considered significant.

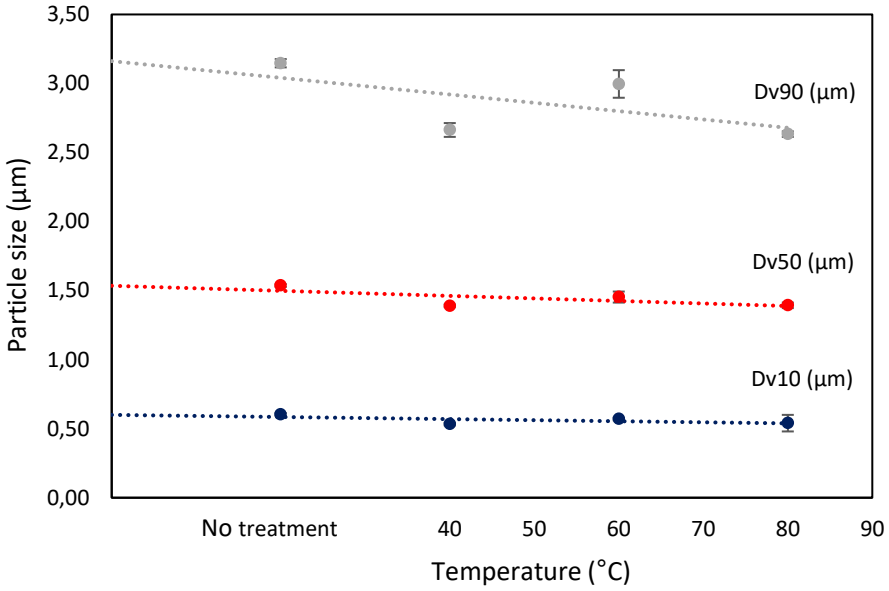

Figure 3.16: Graph of particle size, summarized in Dv10, Dv50 and Dv90, for APIs IH04C with no treatment and with a treatment in conventional oven for 24h at the temperature of 40°C, 60°C and 80°C. The error bars represent the standard deviation based on n=3.

Specific surface area (SSA)

As mentioned before, it was expected that C grade would have a lower SSA due to its smoother surfaces and according to the SEM images. The fact the morphology differences between the 5 samples are tenuous and the error of ± 1 m^2/g of the equipment can contribute to the contrary result: IH04C presented a higher SSA than IH04M (Figure 3.17). The SSA results were then considered inconclusive.

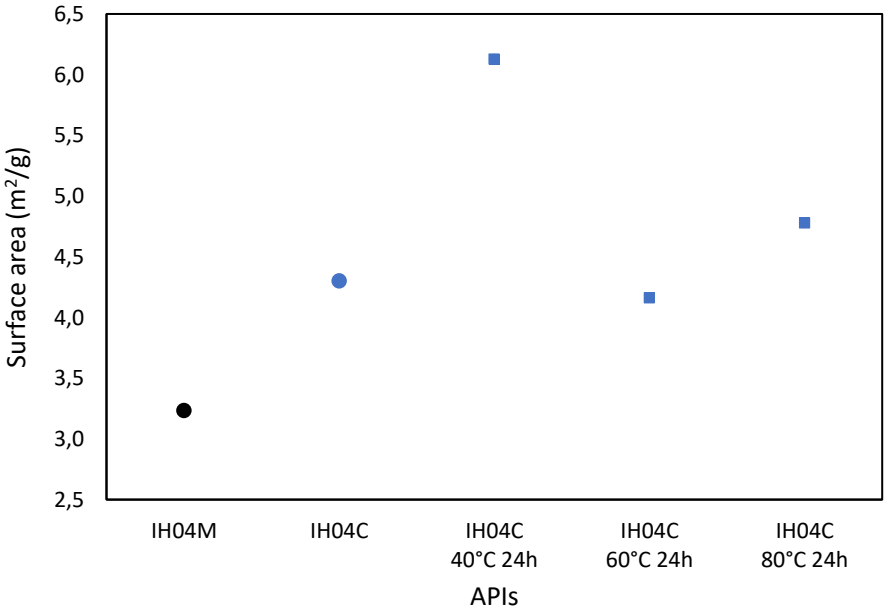

Figure 3.17: Specific surface area obtained by BET for IH04M, IH04C and IH04C 40 °C 24 h, IH04C 60 °C 24 h and IH04C 80 °C 24 h.

X-ray Powder Diffraction (XRPD)

As it can be observed on Figure 3.18, Figure B.15, Figure B.16, Figure B.17 and Figure B.18, independently of the temperature treatment, both the crystallinity and the polymorphic form were not impacted. This is a desirable result since the goal is to alter only the surface properties. It is also possible to observe that the C grade presented a higher crystallinity level than the M grade.

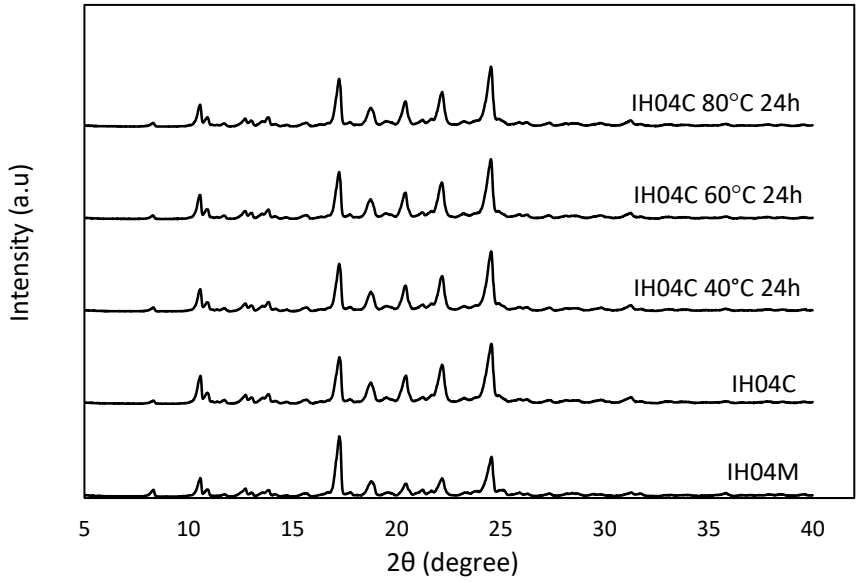

Figure 3.18: X-Ray diffractograms of IH04M, IH04C, IH04C 40 °C 24 h, IH04C 60 °C 24 h and IH04C 80 °C 24 h.

Differential Scanning Calorimetry (DSC)

The DSC technique was used in order to evaluate the thermophysical properties of the APIs. The thermograms in Figure 3.19 present a melting endothermic peak at ~124 ºC followed by a smaller endothermic peak at ~138 ºC. According to the literature, the API undergoes a polymorphic transformation from form I to form II. The absent of recrystallization peak in form II and the low intensity of the melting peak of form II may be related to a high ramping heat and a low conversion [see prior note]. The thermograms are all identical and so the temperature treatment did not modify the thermal behavior of the API.

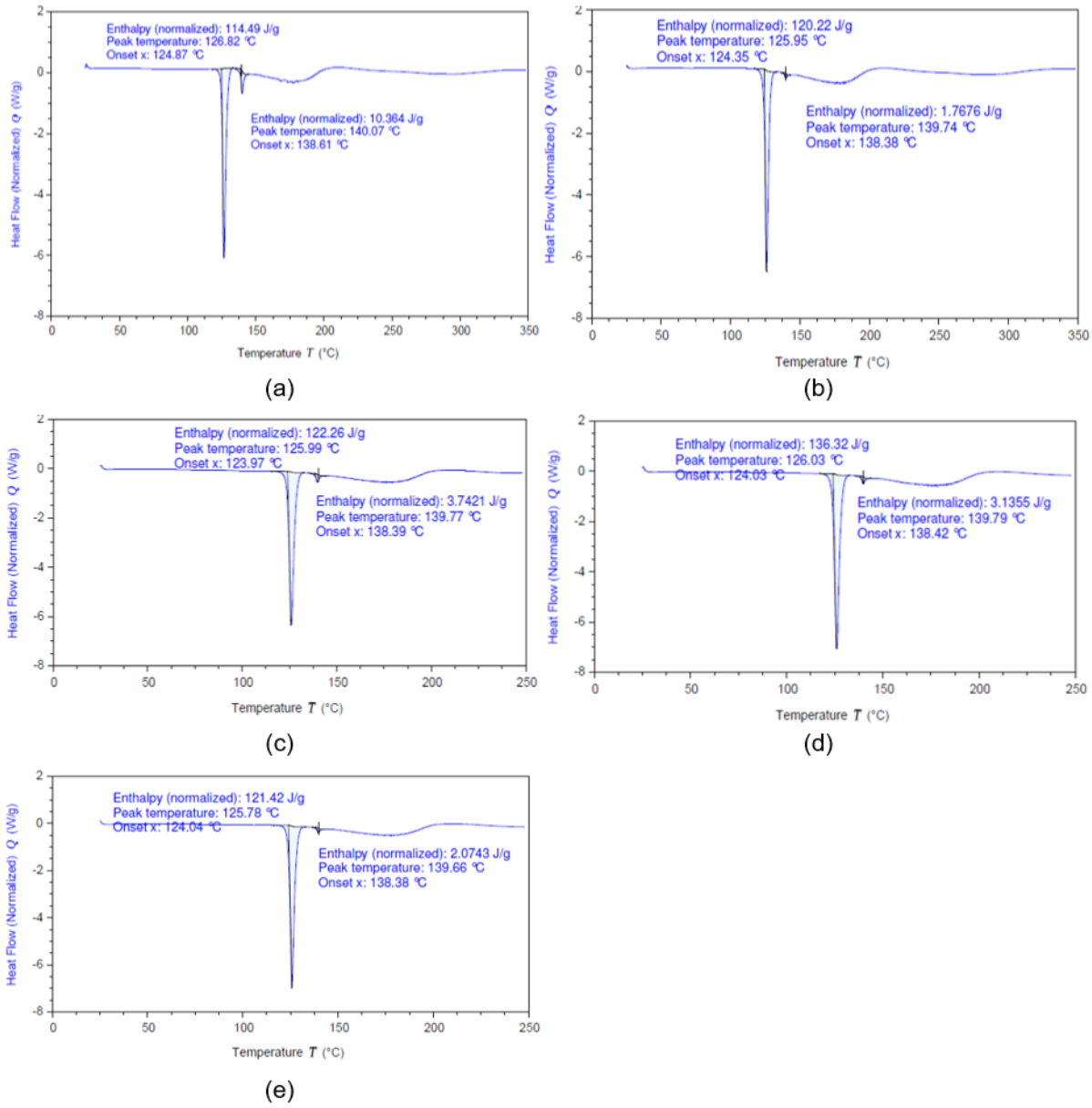

Figure 3.19: Differential scanning calorimetry thermograms of (a) IH04M; (b) IH04C; (c) IH04C 40°C 24h; (d) IH04C 60°C 24h; (e) IH04C 80°C 24h.

Atomic Force Microscopy (AFM)

IH04M shows slightly higher adhesion force than IH04C (Figure 3.20). This can be related to the not so accentuated differences in morphology between C and M grade particles in IH04 as for ST75 and there are no evidences in the manufacturing process that IH04M shows less adhesion to surfaces than IH04C, as it happens to API ST75. Regarding the modified samples, the temperature treatment increased the adhesion forces and so they became more identical to IH04M as intended (except for IH04C 80 °C 24 h that remained practically the same).

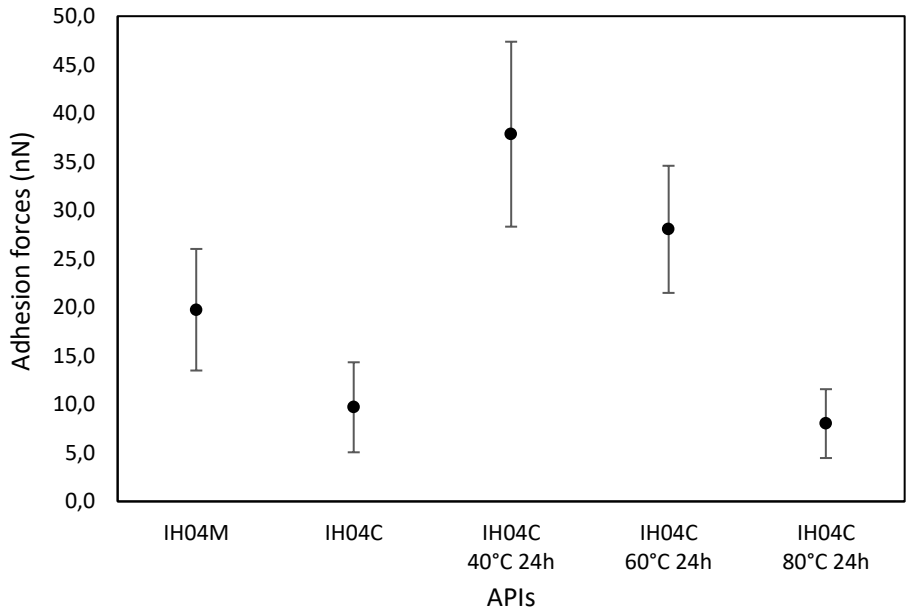

Figure 3.20: Average adhesion forces measured by AFM for API IH04M, IH04C, IH04C 40 °C 24 h, IH04C 60 °C 24 h and IH04C 80 °C 24 h. The error bars represent the standard deviation of all the measurements made on 3 different spots of the sample.

Inverse Gas Chromatography (IGC)

This analysis was not performed to IH04 due to equipment issues during the measurements and the melting of the samples.

3.2.2 Aerodynamic performance

In Figure 3.21 and Figure 3.22 it was visible that API IH04C presents a lower FPF and FPD than IH04M, the same way it happened for the two grades in ST75. Hence, IH04M has the better flowability. The FPF and FPD of modified samples increased in comparison with IH04C becoming more similar to IH04M as intended. The ED of IH04 (Figure 3.23) as it was mentioned for ST75, could have been influenced by the manual method of filling capsules, and so the standard deviations were high. The emitted dose of IH04M was lower than the one of IH04C. From Figure 3.24 it was possible to conclude in which stages the API was deposited and observe the content deposited at the filter, which represents the lowest stages of the lungs (FPD).

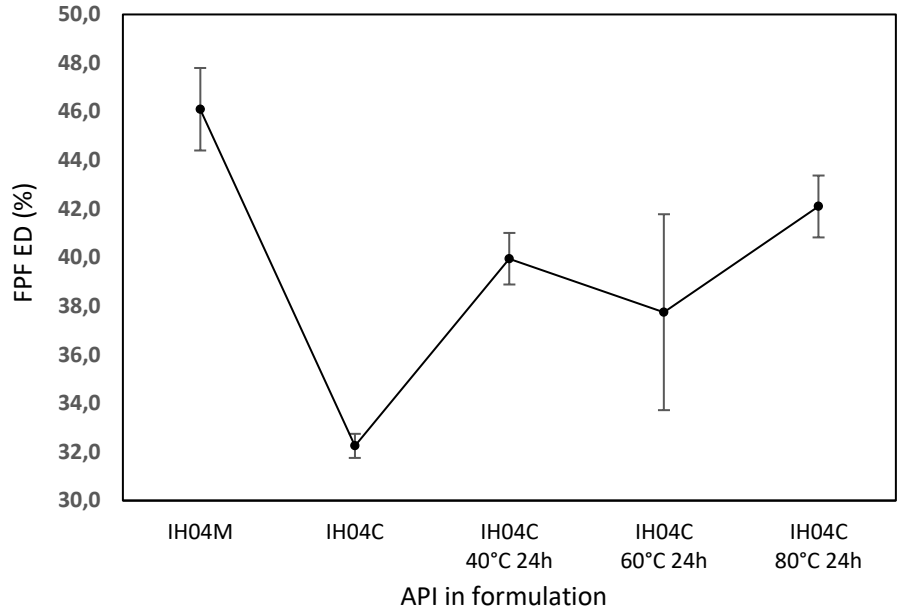

Figure 3.21: Aerodynamic performance evaluation through the FPF (ED) for the blends with the API IH04M, IH04C, IH04C 40°C 24h, IH04C 60°C 24h and IH04C 80°C 24h. The error bars represent the standard deviation based on n=2.

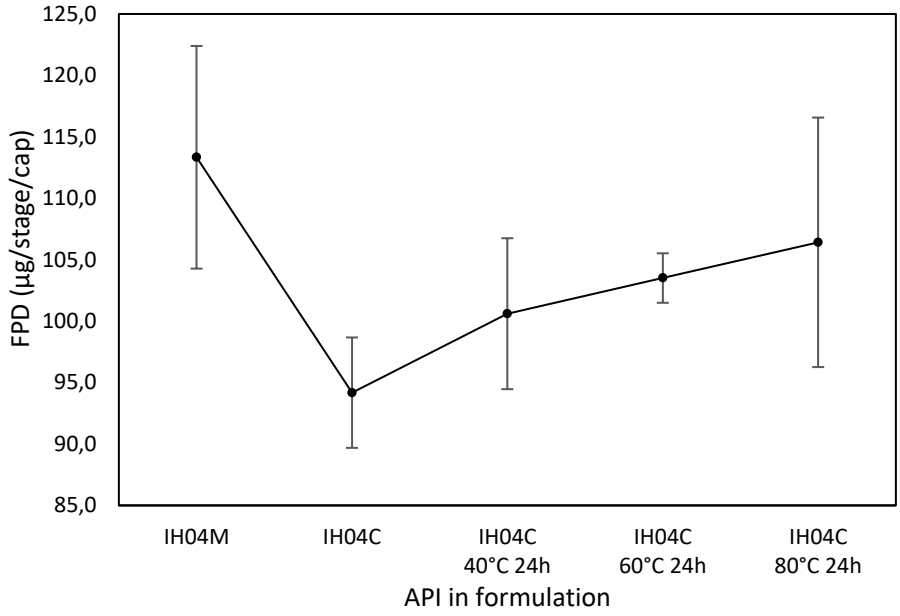

Figure 3.22: Aerodynamic performance evaluation through FPD for the blends with the API IH04M, IH04C, IH04C 40°C 24h, IH04C 60°C 24h and IH04C 80°C 24h. The error bars represent the standard deviation based on n=2.

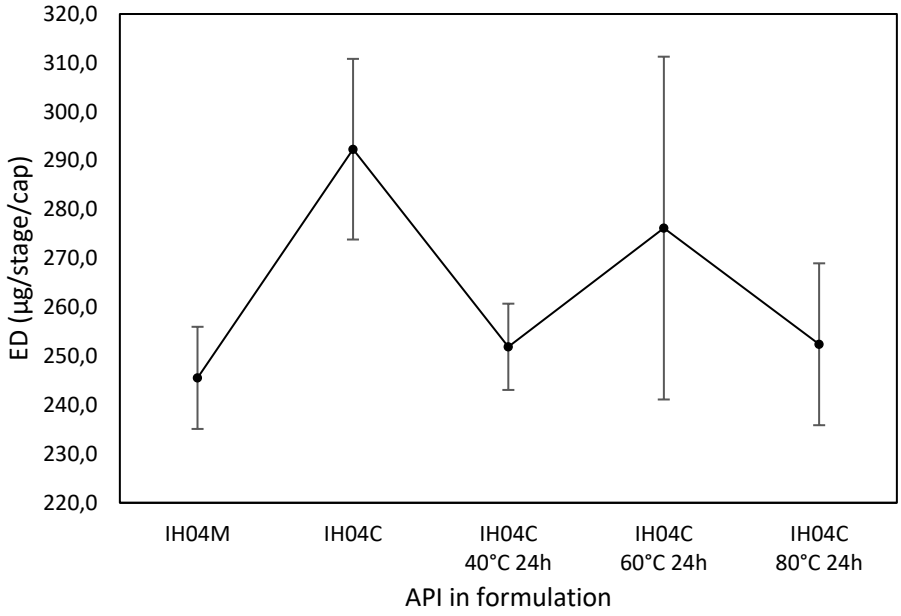

Figure 3.23: Aerodynamic performance evaluation through the ED for the blends with the API IH04M, IH04C, IH04C 40°C 24h, IH04C 60°C 24h and IH04C 80°C 24h. The error bars represent the standard deviation based on n=2.

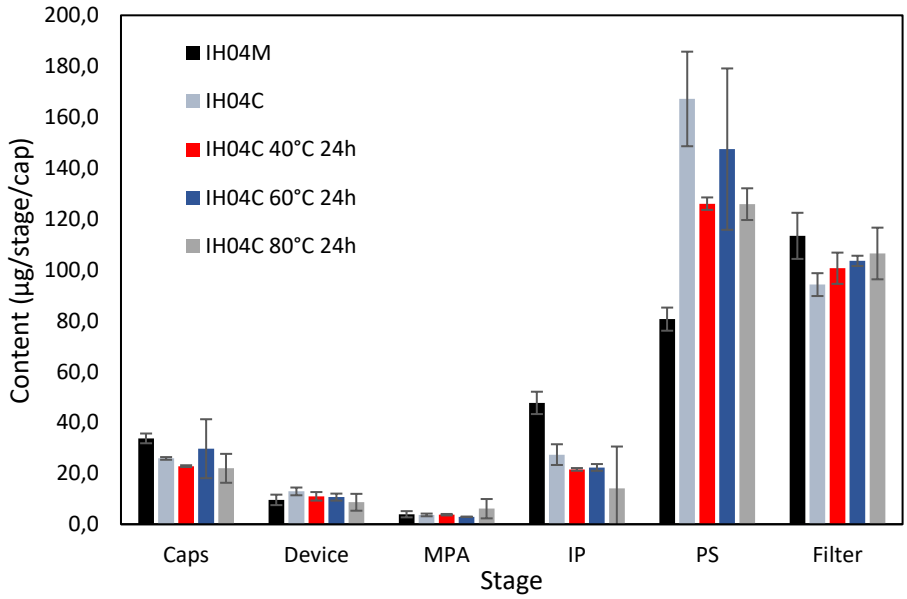

Figure 3.24: Aerodynamic performance evaluation through the content in each stage of the FSI for the blends with the API IH04M, IH04C, IH04C 40 °C 24 h, IH04C 60 °C 24 h and IH04C 80 °C 24 h. The error bars represent the standard deviation based on n=2.

CHAPTER 4

Conclusions and Future Perspectives

The work addressed in this thesis intended to improve the properties of the inhalation particles produced by WP trough different types of treatments in order to make them have a similar behavior to the ones micronized by JM. To achieve this goal, several steps had to be performed: the characterization of API before the surface treatments; the surface modification by a conventional oven and UV-ozone systems, the characterization of the particles after the treatments and finally the aerodynamic performance evaluation. All the steps were performed and concluded with success.

The characterization performed by SEM allowed to conclude that for both APIs, the C grade presented a more polished shape and a smoother surface, when comparing with the M grade, which has a rougher surface. The difference in surface asperities between the grades is more evident for the API ST75. Regarding the conventional oven treatment, in general, as the time of treatment increases, the roughness of the particles surfaces seemed to increase. However, for ST75C, the treatment at 80 °C seemed to yield the same surface asperities at the different time points. This can suggest that the surface achieved a maximum roughness at this temperature and increasing the duration of the treatment did not enhance the irregularities at the surface. The UV-ozone system samples exhibited an increase in surface roughness but changed their color, from white to yellow, and due to possible impurities growth, these samples were not chosen to proceed for the characterization and aerodynamic steps. As future studies, other conditions of treatments at UV-ozone system could be tested and the impurities could be evaluated by HPLC. The group of samples that were chosen to continue the studies was constituted by the samples treated at the conventional oven at 40 ºC, 60 ºC and 80 ºC, during 24 h.

The PSD results remained very similar before and after the treatment. The XRPD and DSC data also remained unchanged before and after the surface modification, so the crystallinity and thermal behavior was not influenced by the treatment. This was a desirable result since the goal was to change only the surface properties without interfering on the remaining properties of the API.

SSA obtained by BET method indicated that C grade had higher SSA than M grade for both APIs, contrary to what was expected based on SEM results. This can be due to the equipment error of ± 1 m^2/g of the measurements that is considerable high taking into account the low value of SSA obtained for the APIs of this study. Taking this into account none of the results were conclusive in terms of surface roughness. As future perspectives, other techniques, such as laser profilometry, could be used to analyse surface roughness.

It was very challenging to extract the adhesion forces results from AFM. ST75C presented higher adhesion force than ST75M as it was expected, being in accordance with the SEM images (i.e., a rougher surface has less adhesion force) and the modified samples had a decrease in adhesion forces becoming more similar to ST75M. For IH04 the modified samples results become closer to IH04M (except for IH04C 80 °C 24 h) but between C and M grades the results for IH04 were opposite of the ones in ST75. This can be due to the tenuous differences in their morphology and the behaviour for this API can be different since there were no evidences in the manufacturing process that indicates IH04M adheres less to surfaces than IH04C. The AFM technique presented a large deviation between measurements and in order to ascertain if AFM is a reliable technique to study these powders, more measurements should be performed.

Through IGC measurements, it was not possible to identify any significant differences between dispersive components of surface energy between the 5 samples, since the error associated to the measurements is 2 mJ m^{-2} and the values were very similar. The powders showed a stronger interaction with the amphoteric probe, indicating they can interact as acid or base, having an amphoteric character. When comparing the affinity to basic or acid probes, the samples showed more interaction with basic probes. Through IGC was not possible to conclude that the modified samples were becoming more similar to M grade than with C grade.

During the aerodynamic performance study, it was possible to infer that for both APIs, that M grade enables a higher FPF than the C grade. The surface roughness modification allowed an increase in FPF relative to C grade, hence it improved their flowability. The FPD and ED had large standard deviations, which can be associated to the small number of replicates (only 2) due to the amount of time required to each measurement, and also because the capsules were hand filled. As future development, the increase on the number of replicates could increase the statistical significance. The use of nanocellulose as excipient can be suggested for future studies, since the material has unique properties and potential for different fields.

In general, the conventional oven treated samples revealed a surface modification by SEM, an approximation to the M grade adhesion forces assessed by AFM, an improvement in the dispersion characteristics through FSIs, and lastly, did not impact on the PSD, crystallinity and thermal behaviour as desired. Furthermore, it is an available technology at Hovione FarmaCiência SA and easily scalable to batch production. Taking this into account the work elaborated pointed to the conventional oven as a promising technique to improve the APIs characteristics.

In order to better understand how the temperature and the duration of the treatment is influencing the physicochemical properties of APIs, the study could comprise more temperatures of treatment and time points and more statistical significance could be aid by increasing the number of measurements made. Other surface techniques can be studied, such as photonic curing; and the aerodynamic performance of the formulations can also be evaluated for MDIs.

Bibliography

[1] T. Peng *et al.*, “Influence of physical properties of carrier on the performance of dry powder inhalers,” *Acta Pharm. Sin. B*, vol. 6, no. 4, pp. 308–318, 2016.

[2] R. Kandasamy and K. Chandrasekaran, “SUSTAINED RELEASE AEROSOL FOR PULMONARY DRUG DELIVERY SYSTEM: A REVIEW,” 2013.

[3] World Health Organization, “Definition of Active Pharmaceutical Ingredient,” 2011.

[4] M. J. Telko and A. J. Hickey, “Dry powder inhaler formulation,” *Respir. Care*, vol. 50, no. 9, pp. 1209–1227, 2005.

[5] G. Pilcer and K. Amighi, “Formulation strategy and use of excipients in pulmonary drug delivery,” *Int. J. Pharm.*, vol. 392, no. 1–2, pp. 1–19, 2010.

[6] D. R. Hess, “Nebulizers: principles and performance.,” *Respir. Care*, vol. 45, no. 6, pp. 609–22, Jun. 2000.

[7] J. B. Fink, G. L. Colice, and R. Hodder, “Inhaler Devices for Patients with COPD,” *COPD J. Chronic Obstr. Pulm. Dis.*, vol. 10, no. 4, pp. 523–535, Aug. 2013.

[8] Fda, Cder, Yeaton, and Ayse, “Metered Dose Inhaler (MDI) and Dry Powder Inhaler (DPI) Products-Quality Considerations Guidance for Industry DRAFT GUIDANCE.”

[9] P. L. Ariyananda, J. E. Agnew, and S. W. Clarke, “Aerosol delivery systems for bronchial asthma,” *Postgrad. Med. J.*, vol. 72, no. 845, pp. 151–156, 1996.

[10] W. H. Ramadan and A. T. Sarkis, “Patterns of use of dry powder inhalers versus pressurized metered-dose inhalers devices in adult patients with chronic obstructive pulmonary disease or asthma: An observational comparative study,” *Chron. Respir. Dis.*, vol. 14, no. 3, pp. 309–320, 2017.

[11] C. Moura, F. Neves, and E. Costa, “Impact of jet-milling and wet-polishing size reduction technologies on inhalation API particle properties,” 2016.

[12] H. A. Kubavat, J. Shur, G. Ruecroft, D. Hipkiss, and R. Price, “Investigation into the Influence of Primary Crystallization Conditions on the Mechanical Properties and Secondary Processing Behaviour of Fluticasone Propionate for Carrier Based Dry Powder Inhaler Formulations,” *Pharm. Res.*, vol. 29, no. 4, pp. 994–1006, Apr. 2012.

[13] H. J. Lee *et al.*, “Preparation and physicochemical characterization of spray-dried and jet-milled microparticles containing bosentan hydrate for dry powder inhalation aerosols,” *Drug Des. Devel. Ther.*, vol. 10, pp. 4017–4030, 2016.

[14] B. Breneman, “Effect of Size Reduction Parameters in Pharmaceutical Manufactering Process,” no. December 2011, 2011.

[15] R. Patel, A. Baria, and N. Patel, “An overview of size reduction technologies in the field of pharmaceutical manufacturing,” *Asian J. Pharm.*, vol. 2, no. 4, p. 216, 2009.

[16] Z. H. Loh, A. K. Samanta, and P. W. Sia Heng, “Overview of milling techniques for improving the solubility of poorly water-soluble drugs,” Asian J. Pharm. Sci., vol. 10, no. 4, pp. 255–274, 2014.

[17] N. Midoux, P. Hošek, L. Pailleres, and J. R. Authelin, “Micronization of pharmaceutical substances in a spiral jet mill,” *Powder Technol.*, vol. 104, no. 2, pp. 113–120, 1999.

[18] “Jet milling | Hovione FarmaCiência SA.” [Online]. Available: https://www.Hovione FarmaCiênciaSA.com/products-and-services/contract-manufacturing-services/particle-engineering/technologies/jet-milling. [Accessed: 26-Jul-2019].

[19] M. D. Louey, M. Van Oort, and A. J. Hickey, “Aerosol Dispersion of Respirable Particles in Narrow Size Distributions Produced by Jet-Milling and Spray-Drying Techniques,” 2004.

[20] H. Steckel, N. Rasenack, P. Villax, and B. W. Müller, “In vitro characterization of jet-milled and in-situ-micronized fluticasone-17-propionate,” *Int. J. Pharm.*, vol. 258, no. 1–2, pp. 65–75, 2003.

[21] “Wet Polishing | Hovione FarmaCiência SA.” [Online]. Available: https://www.hovione.com/products-and-services/contract-manufacturing-services/particle-engineering/technologies/wet. [Accessed: 26-Jul-2019].

[22] “Spray drying | Hovione FarmaCiência SA.” [Online]. Available: https://www.hovione.com/products-and-services/contract-manufacturing-services/particle-engineering/technologies/spray-drying. [Accessed: 26-Jul-2019].

[23] D. E. Dobry, D. M. Settell, J. M. Baumann, R. J. Ray, L. J. Graham, and R. A. Beyerinck, “A model-based methodology for spray-drying process development,” *J. Pharm. Innov.*, vol. 4, no. 3, pp. 133–142, 2009.

[24] C. J. Aundhia *et al.*, “Spray Drying in the Pharmaceutical Industry-A Review,” *Indo Am. J. Pharm. Res.*, vol. 2011, no. 2, pp. 125–138, 2011.

[25] M. D. Jones *et al.*, “An investigation into the relationship between carrier-based dry powder inhalation performance and formulation cohesive-adhesive force balances,” *Eur. J. Pharm. Biopharm.*, vol. 69, no. 2, pp. 496–507, 2008.

[26] G. Pilcer, N. Wauthoz, and K. Amighi, “Lactose characteristics and the generation of the aerosol,” *Adv. Drug Deliv. Rev.*, vol. 64, no. 3, pp. 233–256, 2012.

[27] I. Parisini, J. L. Collett, and D. Murnane, “Mathematical approach for understanding deagglomeration behaviour of drug powder in formulations with coarse carrier,” *Asian J. Pharm. Sci.*, vol. 10, no. 6, pp. 501–512, 2015.

[28] M. D. Jones and R. Price, “The influence of fine excipient particles on the performance of carrier-based dry powder inhalation formulations,” *Pharm. Res.*, vol. 23, no. 8, pp. 1665–1674,

2006.

[29] X. M. Zeng, G. P. Martin, C. Marriott, and J. Pritchard, “Lactose as a carrier in dry powder formulations: The influence of surface characteristics on drug delivery,” *J. Pharm. Sci.*, vol. 90, no. 9, pp. 1424–1434, 2001.

[30] C. C. V. R. Leite, “Improved particle engineering and DPI formulation for optimal pulmonary delivery,” Faculdade de Ciências e Tecnologias, Universidade Nova de Lisboa, 2016.

[31] C. Copley, “Quality Solutions for Inhaler Testing 2019 EDITION.”

[32] C. Scientific, “Copley Scientific ’ s latest Qbd tool slashes analysis time,” no. November, pp. 1–2, 2008.

[33] A. H. L. Chow, H. H. Y. Tong, P. Chattopadhyay, and B. Y. Shekunov, “Particle engineering for pulmonary drug delivery,” *Pharm. Res.*, vol. 24, no. 3, pp. 411–437, 2007.

[34] M. J. Faber, G. Galati, and J. S. Dinyer, “Handling of Highly Potent Pharmaceutical Compounds Effective strategies for Contract Manufacturing Organizations WHAT IS A HIGHLY POTENT COMPOUND?,” 2014.

[35] B. Mei Jin Tan, C. V. Liew, L. W. Chan, and P. W. S. Heng, “Particle Surface Roughness - Its Characterisation and Impact on Dry Powder Inhaler Performance,” in *Pulmonary Drug Delivery*, Chichester, UK: John Wiley & Sons, Ltd, 2015, pp. 199–222.

[36] Malvern Instruments Limited, “WHITEPAPER :A basic guide to particle characterization.”

[37] F. Podczeck, “The Influence of Particle Size Distribution and Surface Roughness of Carrier Particles on the in vitro Properties of Dry Powder Inhalations,” *Aerosol Sci. Technol.*, vol. 31, no. 4, pp. 301–321, 1999.

[38] H. H. S. Corporation, “DSC Measurement of Pharmaceuticals,” no. 79, pp. 1–2, 2007.

[39] S. V. Vilas, S. N. Dhanpal, and P. S. Jagganath, “Formulation and Evaluation of Combination Dry Powder for Inhalation : Influence of Crystalline Excipient,” vol. 2, no. 1, pp. 437–450, 2013.

[40] R. R. L. De, D. A. C. Albuquerque, T. G. S. Cruz, F. M. Yamaji, and F. L. Leite, “Measurement of the Nanoscale Roughness by Atomic Force Microscopy: Basic Principles and Applications,” *At. Force Microsc. - Imaging, Meas. Manip. Surfaces At. Scale*, 2012.

[41] S. Sousa, J. Pedrosa, A. Ramos, P. J. Ferreira, and J. A. F. Gamelas, “Surface properties of xylan and xylan derivatives measured by inverse gas chromatography,” *Colloids Surfaces A Physicochem. Eng. Asp.*, vol. 506, pp. 600–606, Oct. 2016.

[42] S. Mohammadi-Jam and K. E. Waters, “Inverse gas chromatography applications: A review,” *Adv. Colloid Interface Sci.*, vol. 212, pp. 21–44, Oct. 2014.

[43] D. Murnane, C. Marriott, and G. P. Martin, “Polymorphic control of inhalation microparticles prepared by crystallization,” *Int. J. Pharm.*, vol. 361, no. 1–2, pp. 141–149, Sep. 2008.

[44] SympatecGmbH - System | Partikel | Technik, “HELOS-BR-RODOS-L-ASPIROS.” [Online].

Available: https://www.sympatec.com/en/particle-measurement/sensors/laser-diffraction/helos/helos-br-rodos-l-aspiros/. [Accessed: 26-Jul-2019].

[45] T. Jenkins and M. Waite, “Alliance HPLC,” pp. 5–6.

Appendix A

Complementary Information to Materials and Methods

This appendix provides complementary information that was not included in the chapter Materials and Methods because lack of space.

Figure A.1: Laser particle size analyzer Sympatec HELOS/BR + RODOS/M + ASPIROS. Adapted from [44].

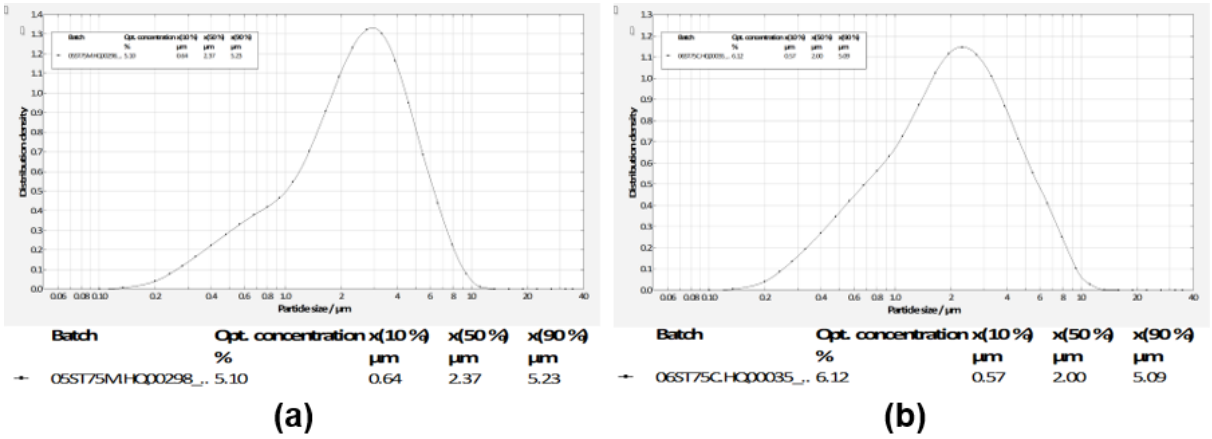

Figure A.2: Particle size distribution curve of input material (a) ST75M and (b) ST75C.

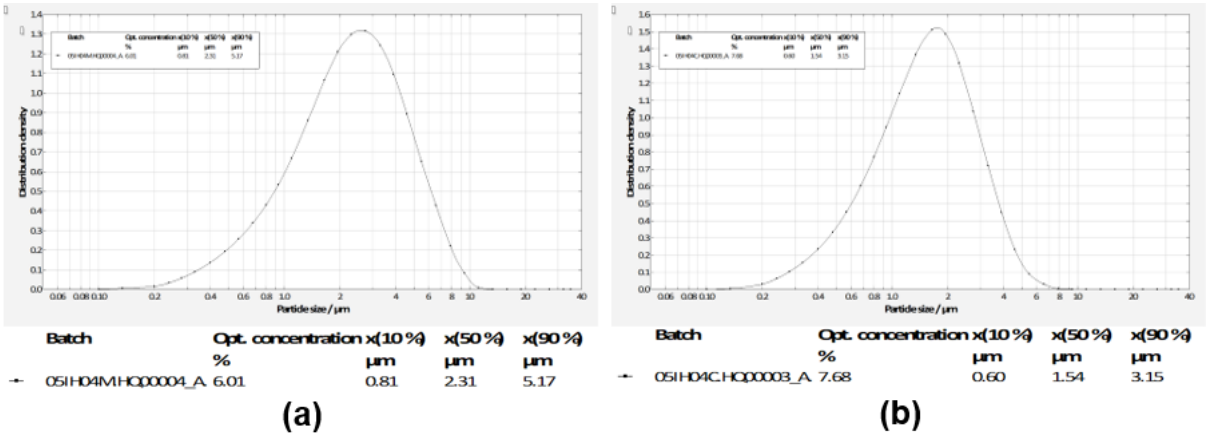

Figure A.3: Particle size distribution curve of input material (a) IH04M and (b) IH04C.

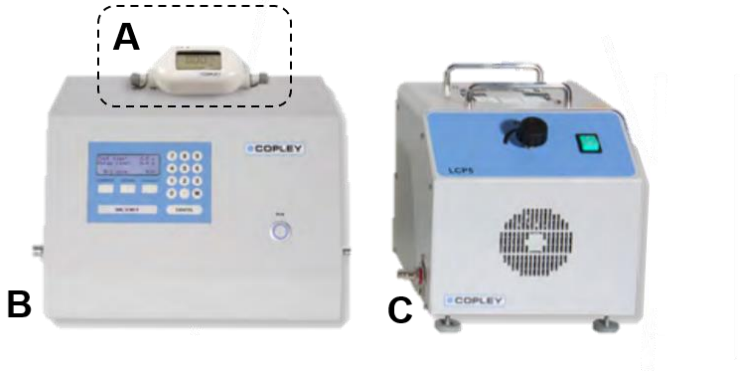

Figure A.4: Complementary equipment of FSI. A - Flowmeter; B - Flow Controller; C - Vacuum pump. Adapted from [32].

Figure A.5: Waters Alliance e2695 HPLC System with Waters 2998 PDA detector. Adapted from [45].

Appendix B

Complementary Information to Results and Discussion

Appendix B contains images and graphics that are part of the chapter Results and Discussion but that were not included because lack of space.

Active Pharmaceutical Ingredient: ST75

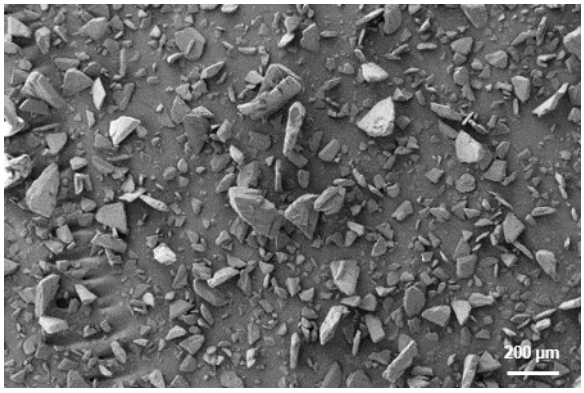

Figure B.1: SEM image of material ST75 not micronized.

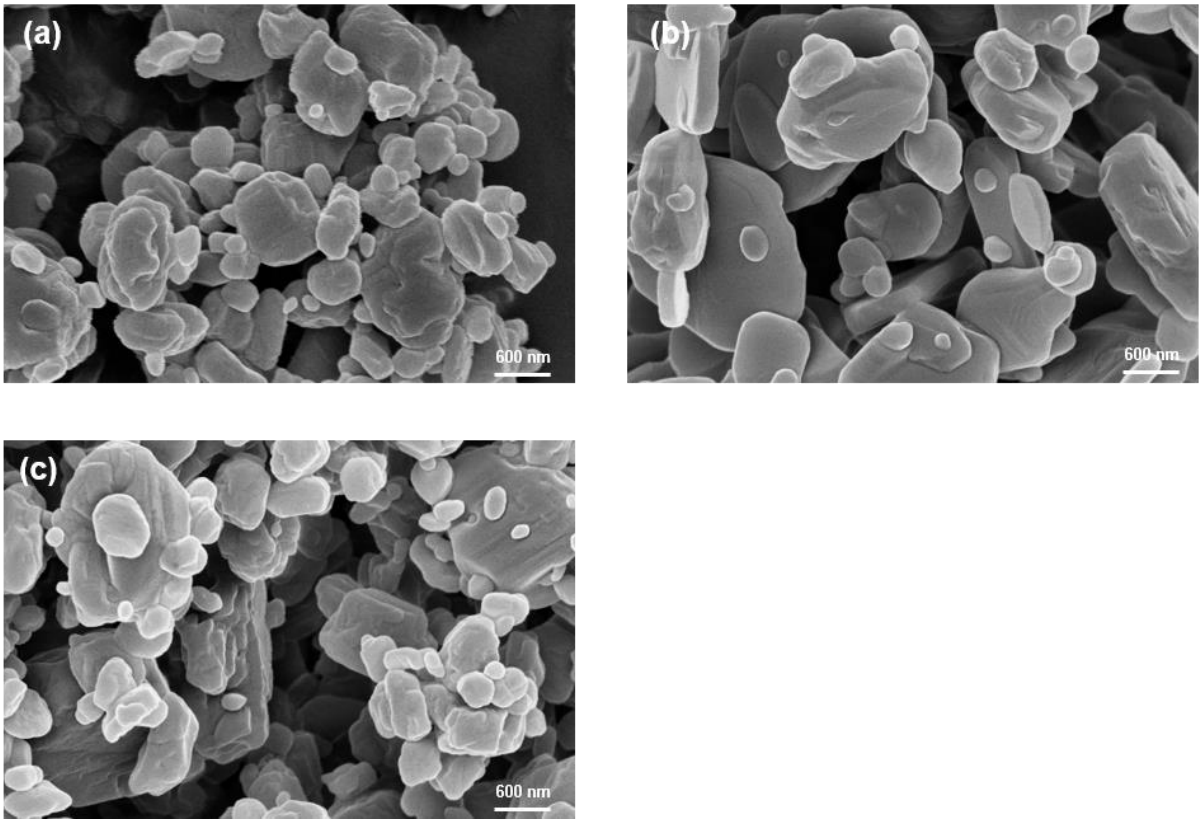

Figure B.2: SEM images of modified samples by conventional oven: (a) ST75C 40 °C 4 h; (b) ST75C 40 °C 8 h; (c) ST75C 40 °C 24 h.

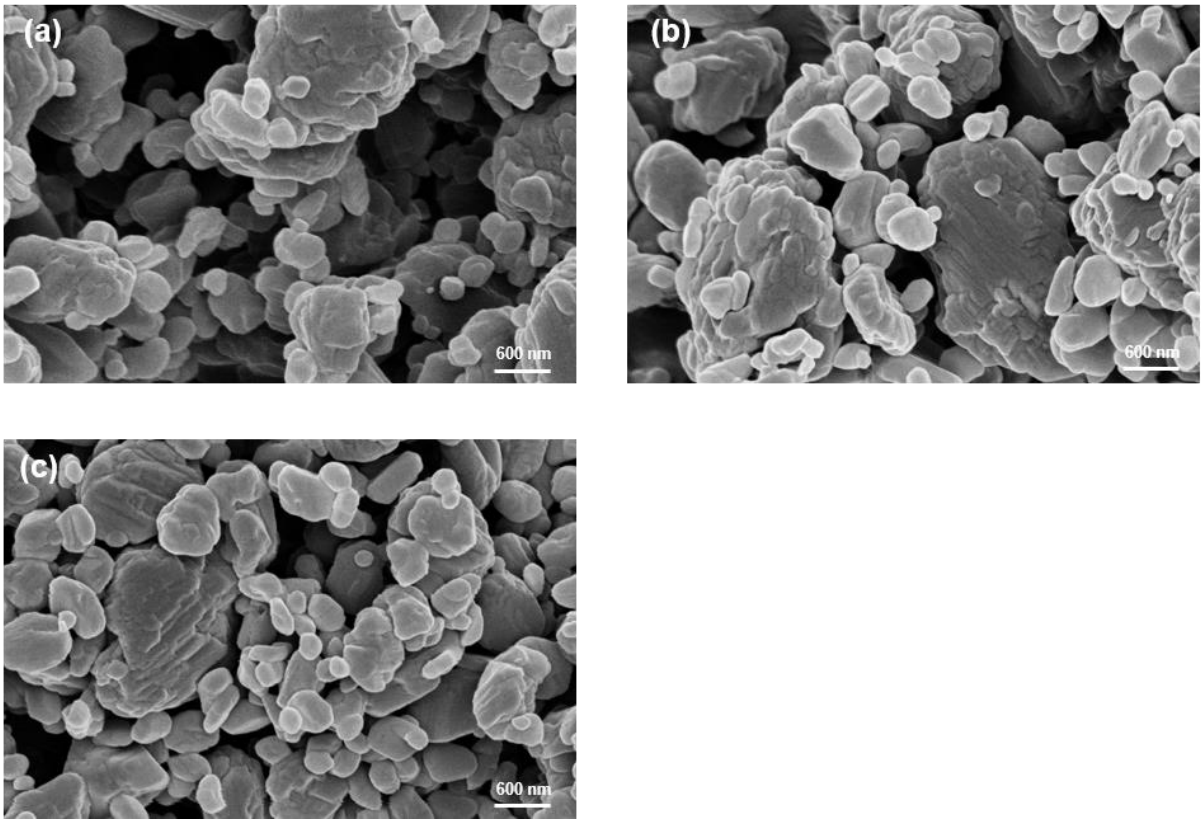

Figure B.3: SEM images of modified samples by conventional oven: (a) ST75C 60 °C 4 h; (b) ST75C 60 °C 8 h; (c) ST75C 60 °C 24 h.

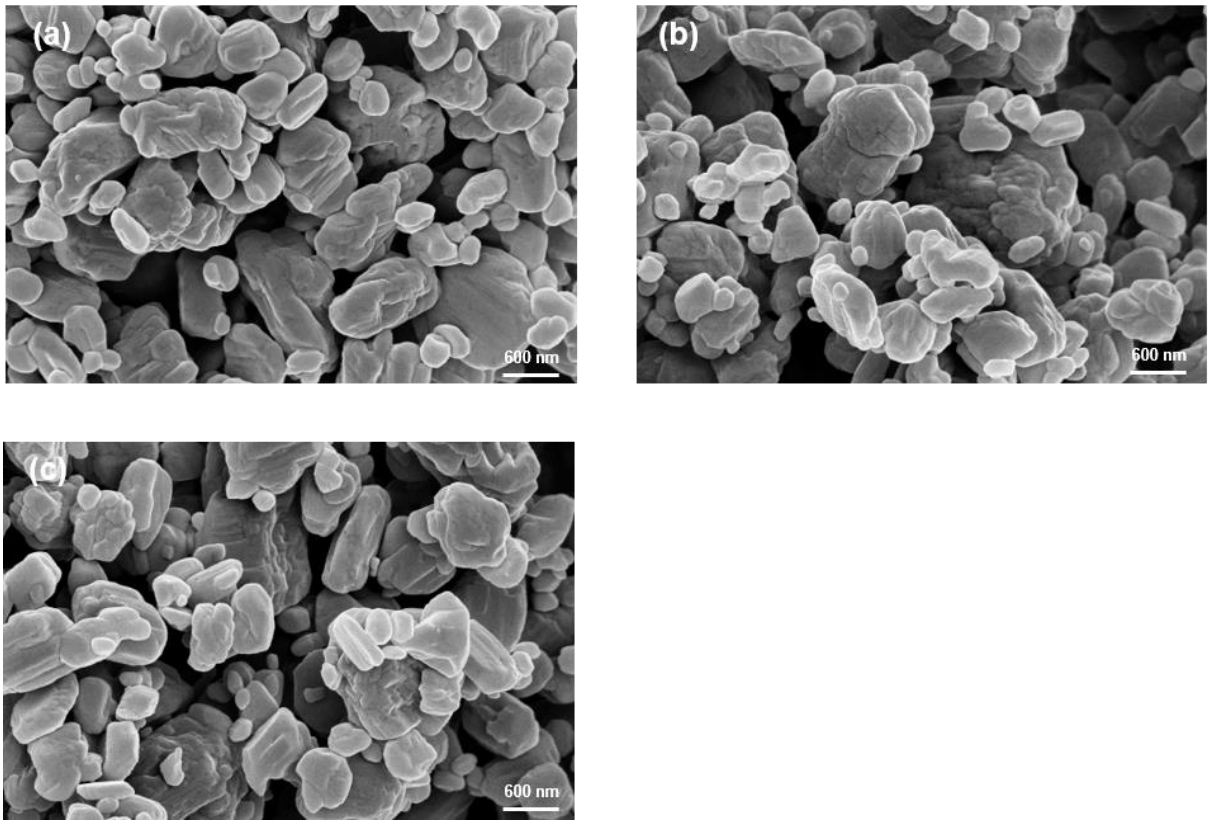

Figure B.4: SEM images of modified samples by conventional oven: (a) ST75C 80 °C 4 h; (b) ST75C 80 °C 8 h; (c) ST75C 80 °C 24 h.

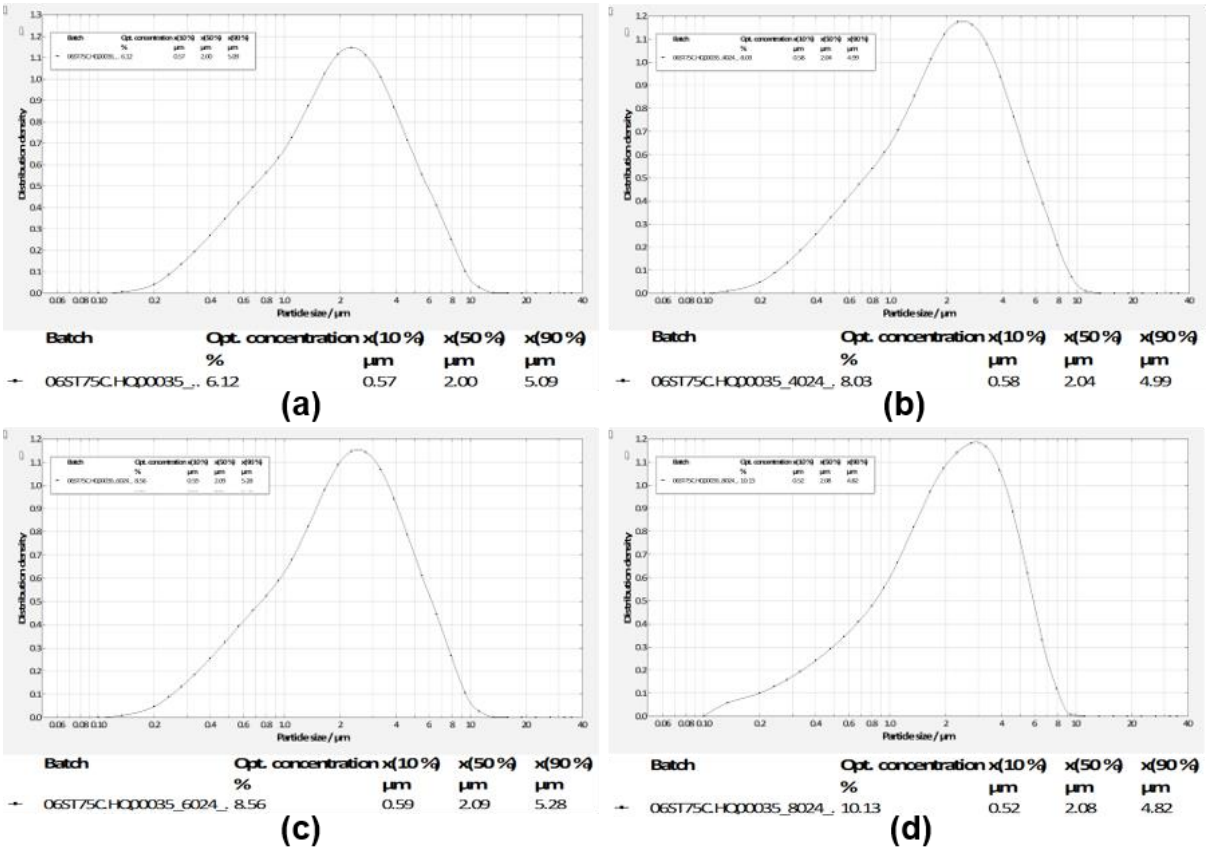

Figure B.5: Particle size distribution curve of input material (a) ST75C (b) ST75C 40 °C 24 h; (c) ST75C 60 °C 24 h; (d) ST75C 80 °C 24 h.

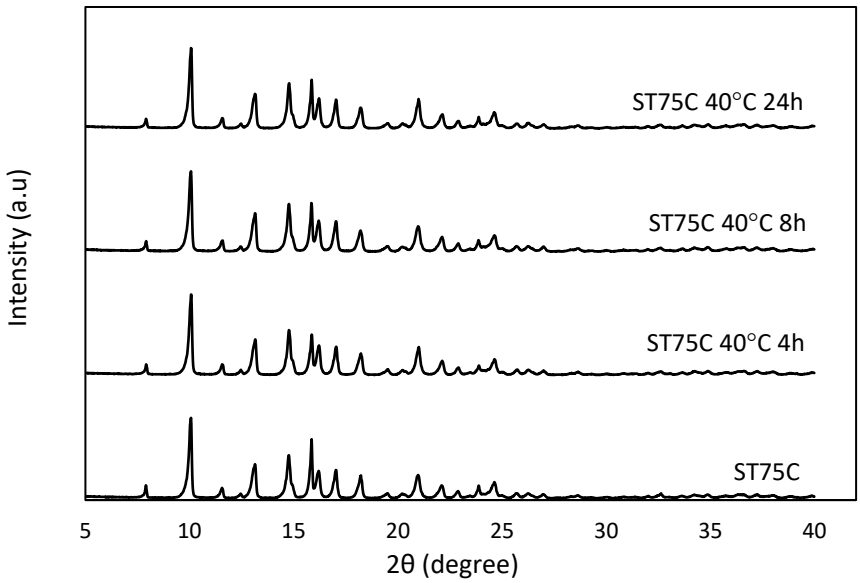

Figure B.6: X-Ray diffractograms of ST75C, ST75C 40 °C 4 h, ST75C 40 °C 8 h and ST75C 40 °C 24 h.

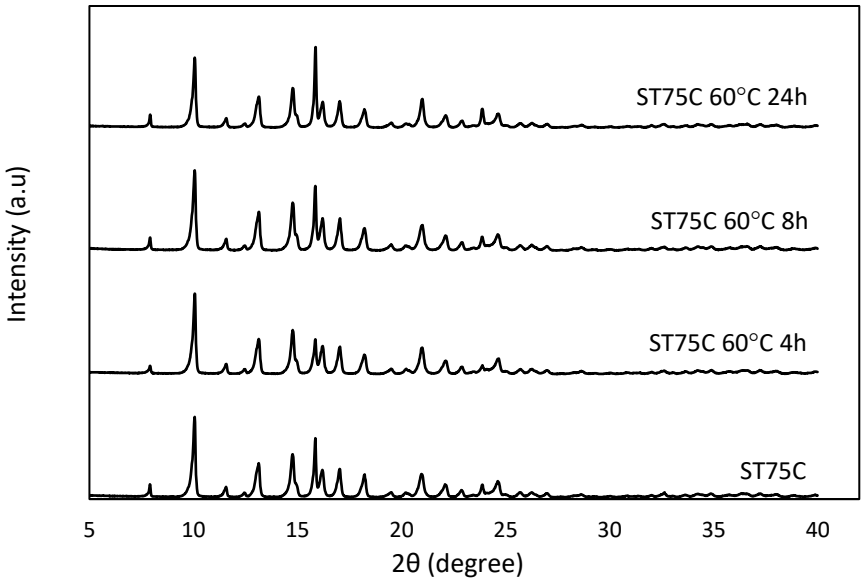

Figure B.7: X-Ray diffractograms of ST75C, ST75C 60 °C 4 h, ST75C 60 °C 8 h and ST75C 60 °C 24 h.

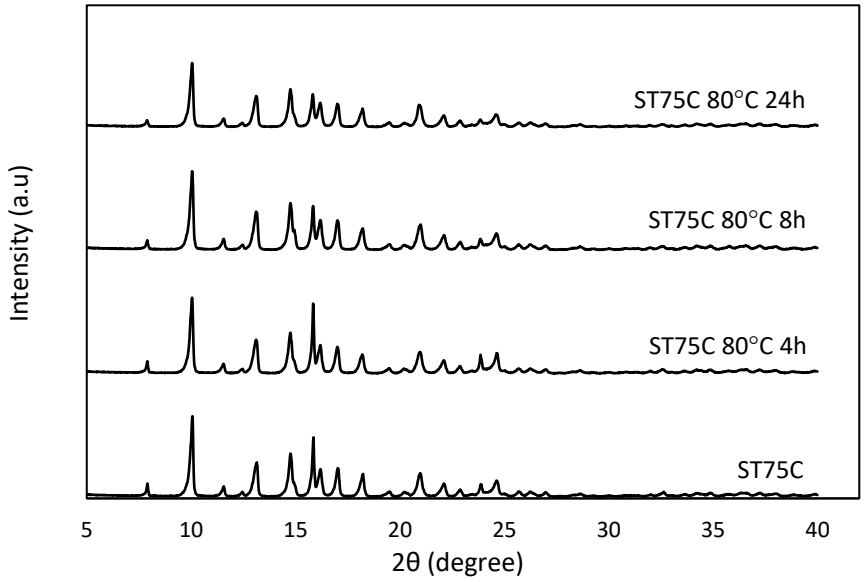

Figure B.8: X-Ray diffractograms of ST75C, ST75C 80 °C 4 h, ST75C 80 °C 8 h and ST75C 80 °C 24 h.

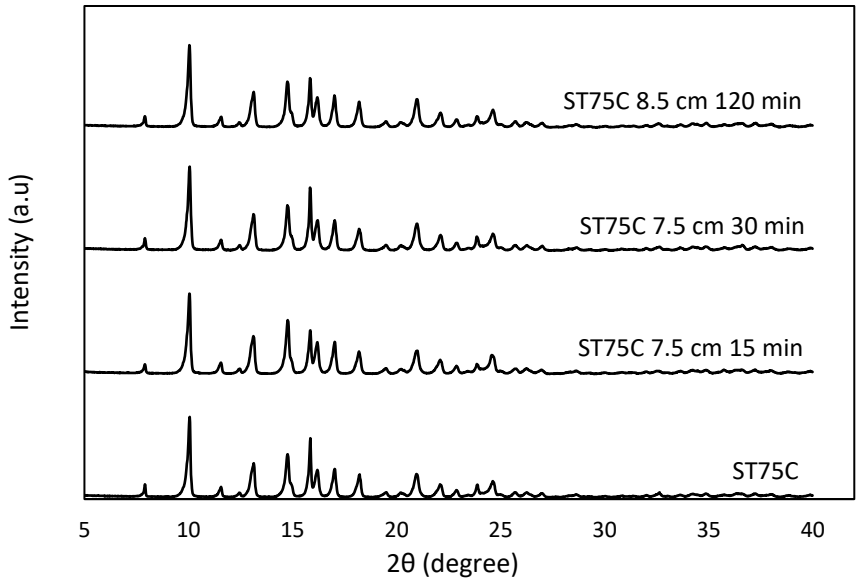

Figure B.9: X-Ray diffractograms of ST75C, ST75C 7.5 cm 15 min, ST75C 7.5 cm 30 min and I ST75C 8.5 cm 120 min.

Active Pharmaceutical Ingredient: IH04

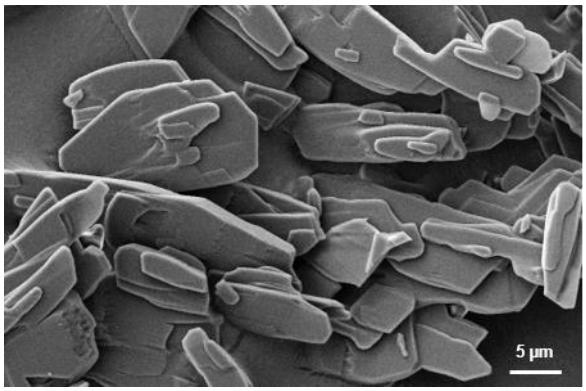

Figure B.10: SEM image of material IH04 not micronized.

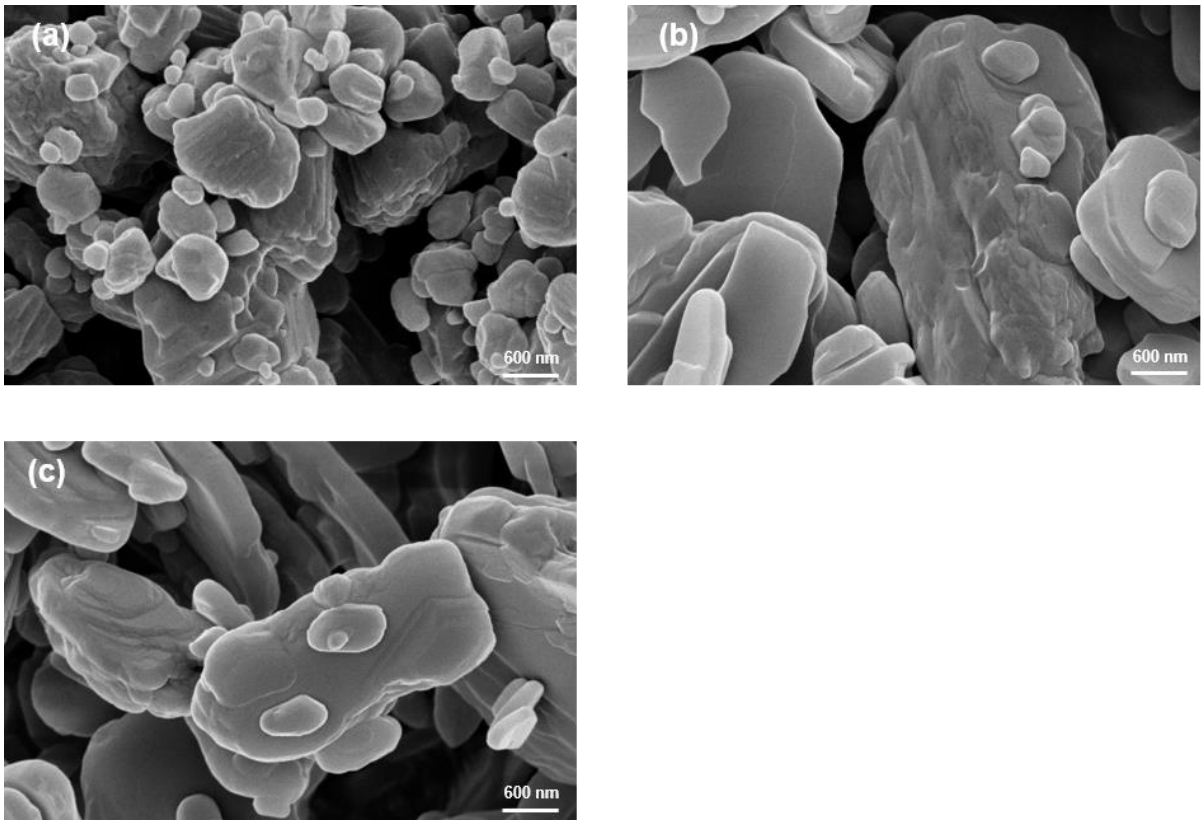

Figure B.11: SEM images of modified samples by conventional oven: (a) IH04C 40 °C 4 h; (b) IH04C 40 °C 8 h; (c) IH04C 40 °C 24 h.

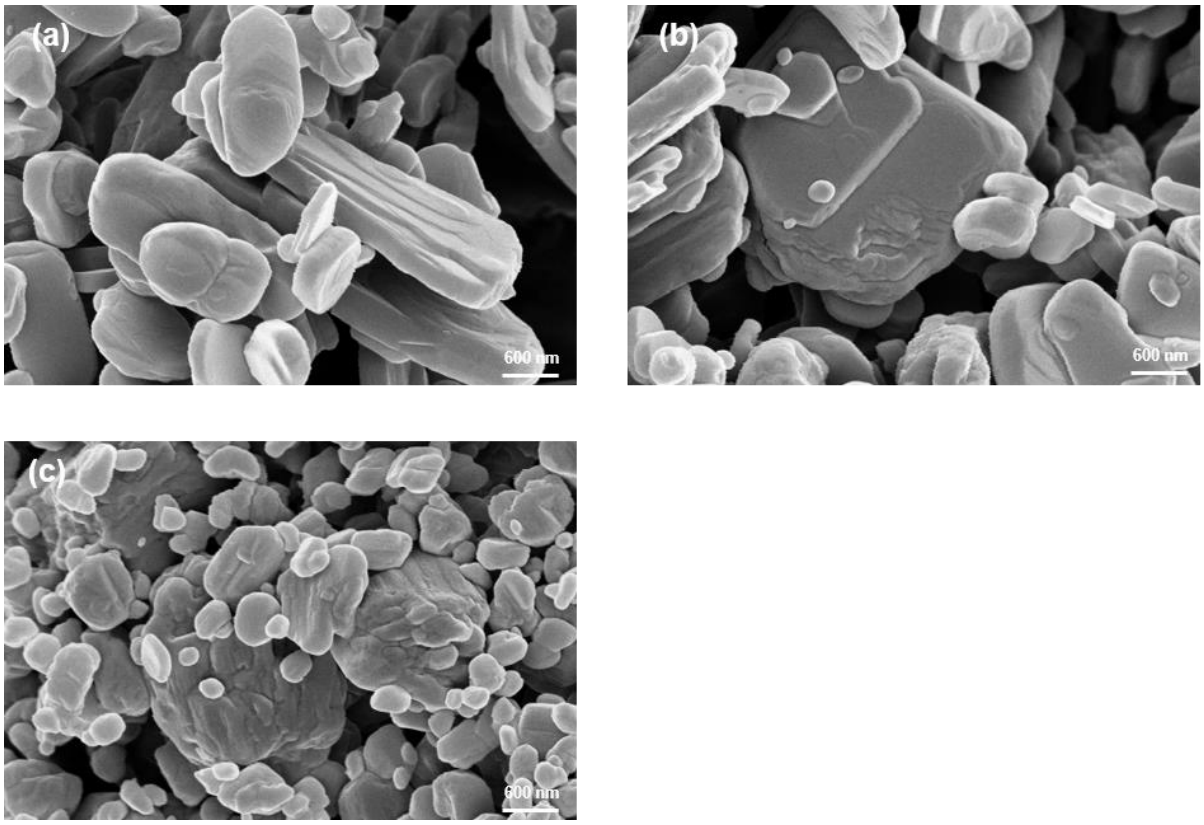

Figure B.12: SEM images of modified samples by conventional oven: (a) IH04C 60 °C 4 h; (b) IH04C 60 °C 8 h; (c) IH04C 60 °C 24 h.

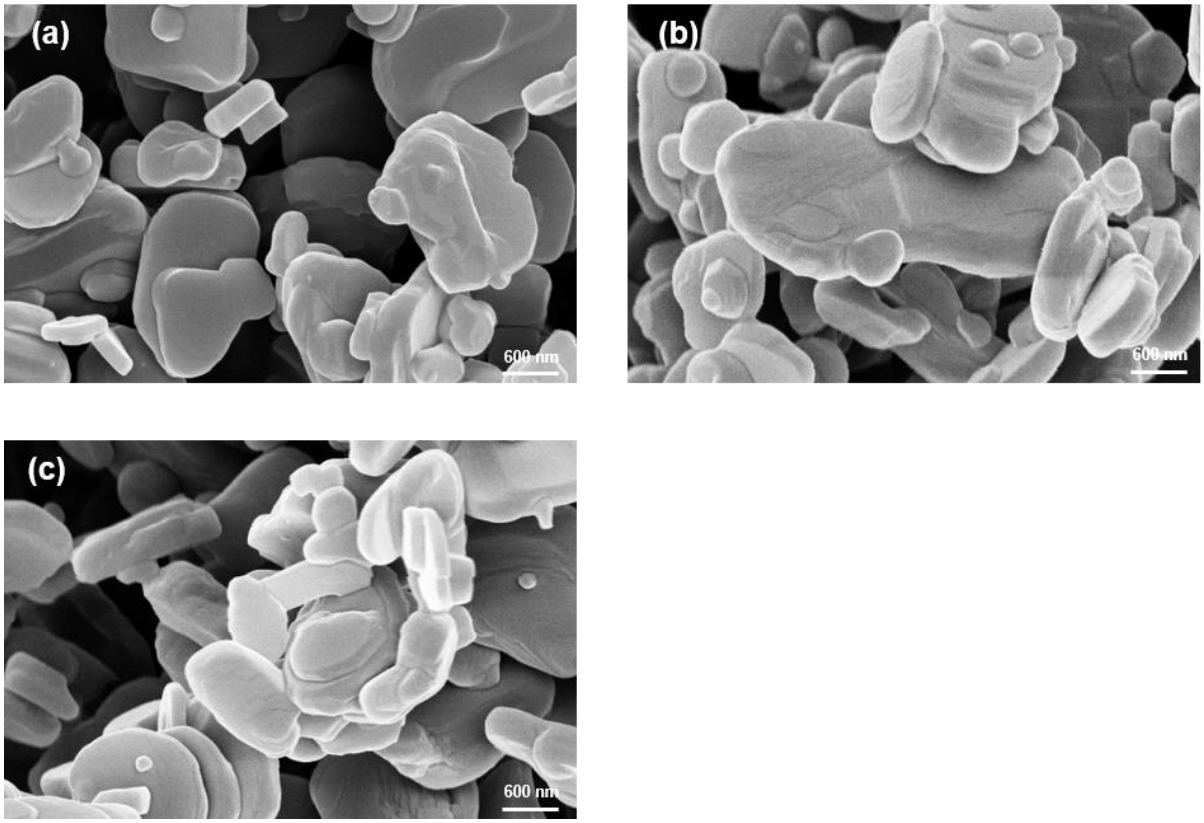

Figure B.13: SEM images of modified samples by conventional oven: (a) IH04C 80 °C 4 h; (b) IH04C 80 °C 8 h; (c) IH04C 80 °C 24 h.

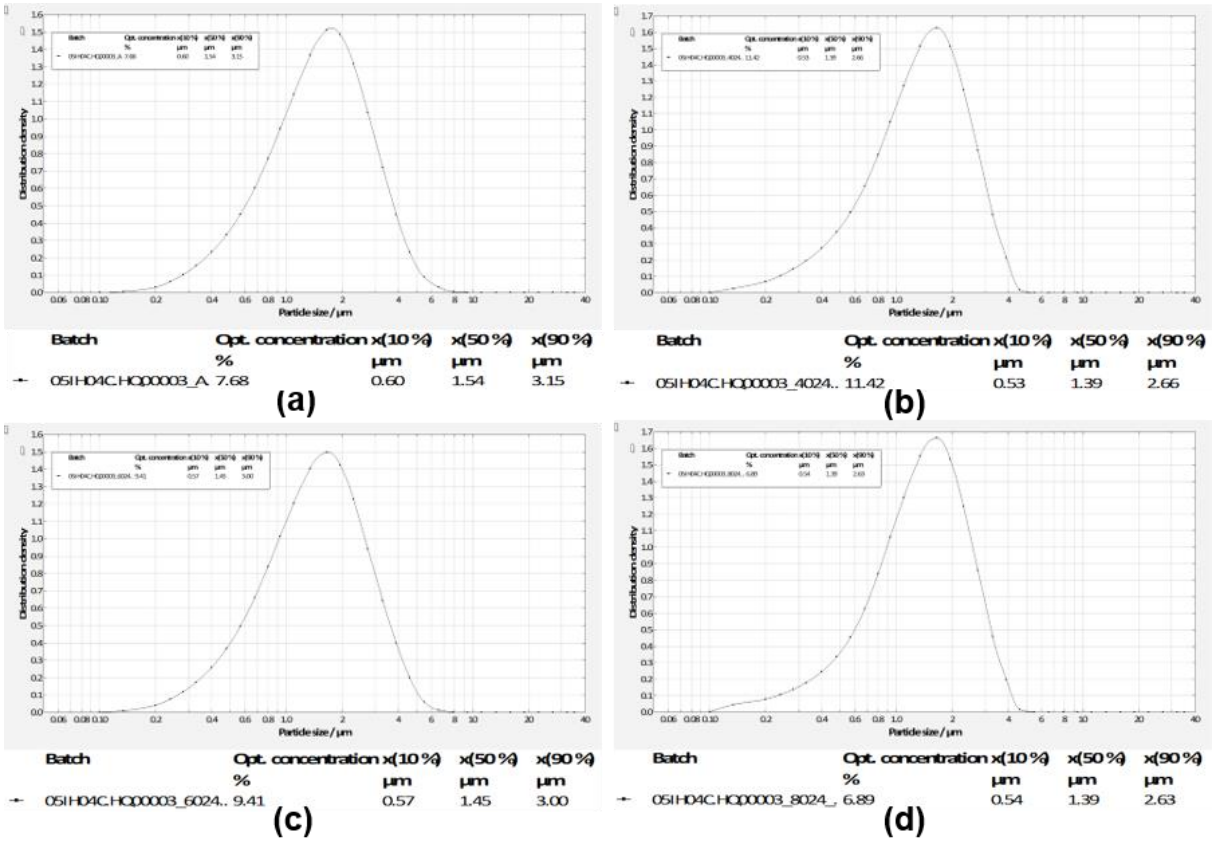

Figure B.14: Particle size distribution curve of input material (a) IH04C (b) IH04C 40 °C 24 h; (c) IH04C 60 °C 24 h; (d) IH04C 80 °C 24 h.

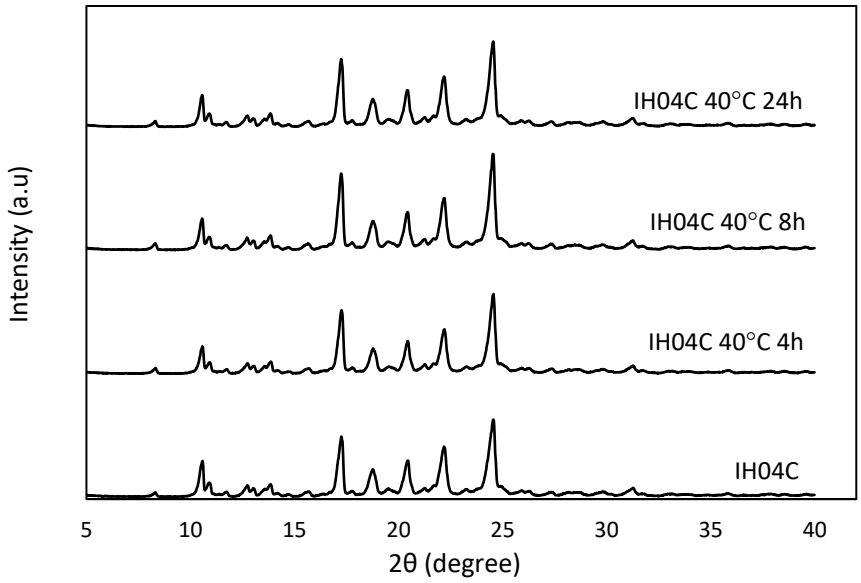

Figure B.15: X-Ray diffractograms of IH04C, IH04C 40 °C 4 h, IH04C 40 °C 8 h and IH04C 40 °C 24 h.

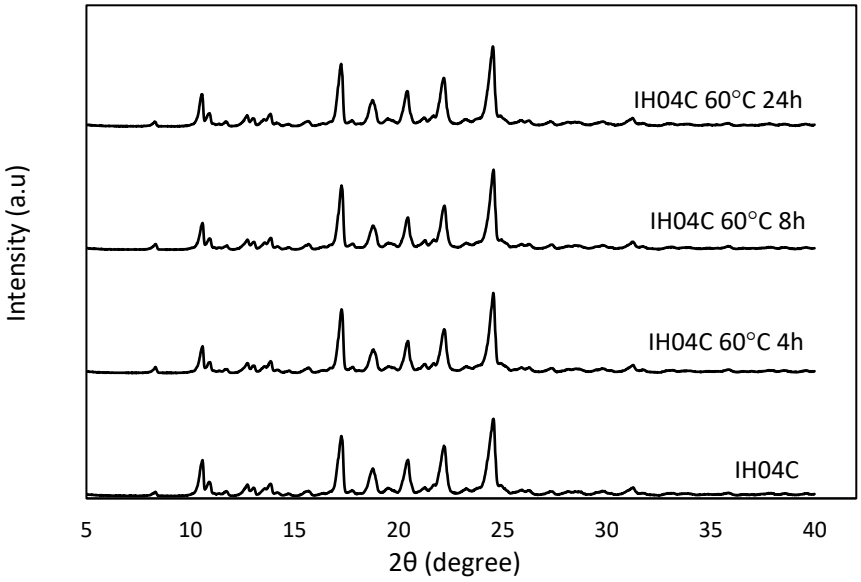

Figure B.16: X-Ray diffractograms of IH04C, IH04C 60 °C 4 h, IH04C 60 °C 8 h and IH04C 60 °C 24 h.

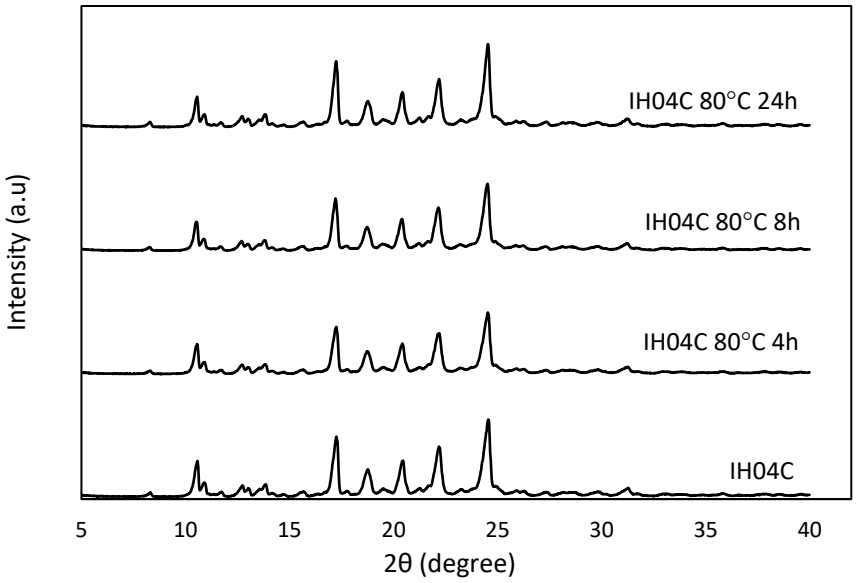

Figure B.17: X-Ray diffractograms of IH04C, IH04C 80 °C 4 h, IH04C 80 °C 8 h and IH04C 80 °C 24 h.

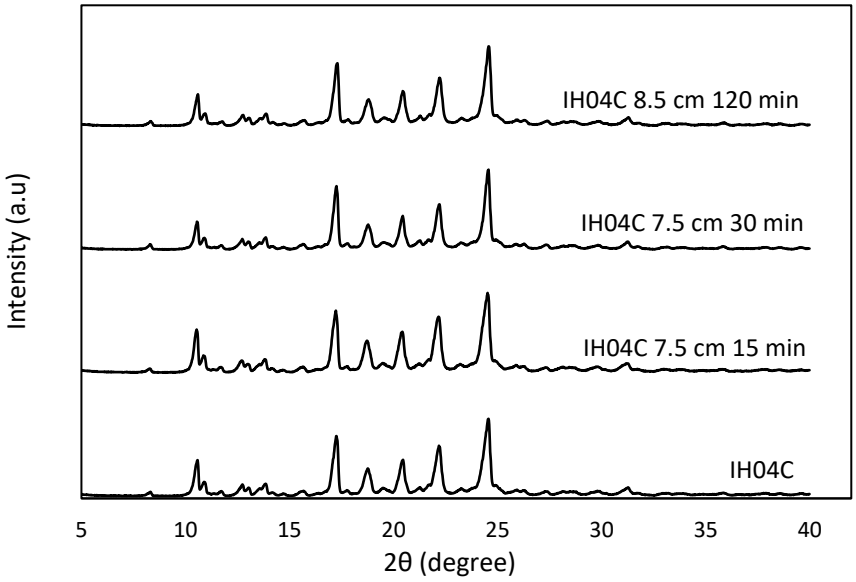

Figure B.18: X-Ray diffractograms of IH04C, IH04C 7.5 cm 15 min, IH04C 7.5 cm 30 min and IH04C 8.5 cm 120 min.